Expert Systems With Applications 229 (2023) 120300

Contents lists available at ScienceDirect

Expert Systems With Applications

journal homepage: www.elsevier.com/locate/eswa

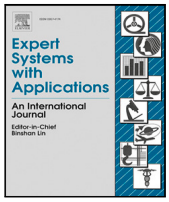

Multiroute fresh produce green routing models with driver fatigue using Type-2 fuzzy logic-based DFWA

Kishore Thakur [a,b,*], Somnath Maji [c], Samir Maity [d,*], Tandra Pal [a], Manoranjan Maiti [e]

[a] Department of Computer Science & Engineering, NIT Durgapur, India
[b] Department of BCA, Midnapore College, India
[c] Department of Computer Science & Engineering, MAKAUT, India
[d] Department of Materials and Production, Operations Research Group, Aalborg University, 9220 Aalborg, Denmark
[e] Department of Applied Mathematics with Oceanology and Computer Programming, Vidyasagar University, West Bengal, India

ARTICLE INFO

Keywords:
Routing
Fresh goods delivery system
Driver's rest
Meta-heuristics
Type-2 fuzzy logic

ABSTRACT

In developing countries, 40 percent of fresh fruits and vegetables are generally transported through nonrefrigerated vehicles and perishes before use, and wholesalers lose potential profits due to item rot. Here, a wholesaler's conveyance with fresh goods starts from a depot and returns to it after dropping the amounts at nodes (retailers) as per previously placed orders. As a perishable item's freshness (color and texture) changes with time, the item's selling price depends on its freshness at the time of delivery to retailers. There are multiple route connections among retailers and depots. Due to fatigue, the driver takes 15 minutes to rest after every two hours during the journey; otherwise, they are at risk of becoming overtired. Under these circumstances, multiroute fresh produce green routing models (MrFPGRMs) are formulated considering the product's freshness, optimum routing plan, appropriate routes, sales revenue, vehicle's running cost and speed, costs and times due to transportation and unloading, fixed charges, greenness (fuel cost), driver's salary and fatigue. The objective is to find the optimum routing plan, best-suited routes between the nodes, and vehicle velocity for the wholesaler's maximum profit, minimum fuel cost, or both. Virgin discrete fireworks algorithms are developed for the solution based on Type-1 and Type-2 fuzzy logic (T1FLDFWA and T2FLDFWA). Numerical experiments are performed through the T2FLDFWA for two time-dependent freshness functions, one of which is new. The results against driver rest, no rest, continuous journey risk, and a trade-off between profit and greenness are presented. Pareto fronts for multiobjectives are depicted. Some managerial decisions are observed.

1. Introduction and motivation

After China, India stands at the top of the production of fruits and vegetables.[1] In 2021–22, India maintained the estimated production of fruits and vegetables at approximately 103 and 200 million tonnes, respectively.[2] As estimated by the United Nations, 12 million tonnes of fruits and 21 million tonnes of vegetables are lost each year.[3] Moreover, approximately $\frac{1}{3}$rd of the total globally produced fruits and vegetables are not up to the standard quality (Gustavsson et al., 2011). Against the immense global demands for these perishable items, it is a very disappointing scenario (Jedermann et al., 2014).

Currently, greenhouse gas emissions (GHGEs) are of great concern for civilization, as global climate change is a severe threat to the world. The transportation sector contributes the largest share of GHGEs, primarily from fossil fuel burning. In 2020, this sector emitted approximately 27% of the total GHGE, which is 5981 million tons in the United States of America.[4] Again, road transportation is not possible without carbon emissions (CEs). For this reason, an attempt is made to adopt a transportation arrangement with minimum CE, which is dependent on the road condition, stoppage at toll plazas, vehicle condition and weight, type of fuel, etc.

It is observed that with the increase in road transport, the number of accidents has increased, mainly due to the driver fatigue. According to Tucker et al. (2003) and Wang and Pei (2014), a driver should take 15 min of rest after every two hours of a continuous journey. To date,

* Corresponding authors.
E-mail addresses: kishore.thakur@midnaporecollege.ac.in (K. Thakur), somnathmajivucs@gmail.com (S. Maji), maitysamir13@gmail.com (S. Maity), tandra.pal@gmail.com (T. Pal), mmaiti2005@yahoo.co.in (M. Maiti).

[1] https://rb.gy/4b9fsl.
[2] https://rb.gy/ic6hcm.
[3] https://rb.gy/dcyw58.
[4] https://urlzs.com/wsErx.

https://doi.org/10.1016/j.eswa.2023.120300
Received 22 October 2021; Received in revised form 11 March 2023; Accepted 26 April 2023
Available online 19 May 2023

there is no drafted routing plan that includes the driver's break. Thus, perishable goods are increasingly wasted, CE increases, and car accidents occur often due to road transportation. These unwanted effects may be due to the lack of a proper plan for distribution/transportation. Therefore, the above problems are significant for the present world and deserve detailed studies in the context of current infrastructural developments across the globe, especially in developing countries.

During the last few years, there have been many infrastructural developments throughout the world. In India, several national highways (NHs) have been built, connecting large and small cities (Raghuram, 2012). Hence, several routes (three-dimensional (3D) transportation) are available to transport goods from one place to another. Moreover, some taxes (monetary) are collected at toll plazas (on NHs) from the plying vehicles to maintain the NHs. Few investigators have formulated 3D routing problems (3DRPs) with several available routes between nodes (cities).

Fresh food products, such as vegetables, fruits, and fishes, gradually deteriorate in the postharvest period. The freshness/acceptability of these items decreases with the time gap between the item's harvesting and delivery (Blackburn & Scudder, 2009). The good's rot plays a negative role in profit-making for both the parties – supplier/wholesaler and retailers – as the selling price of these items is related to freshness.

In the context of the above facts, in developing countries, the delivery of perishable items from a wholesaler to retailers invites several questions: (i) how can the wastage of the perishable items be reduced?, (ii) how can the GHGE be controlled?, (iii) how can items be distributed using available infrastructural facilities for the wholesaler's maximum profit?, and (iv) for a particular routing plan, how much risk (at what level) with respect to (wrt.) Driver fatigue is involved, and (v) how can this real-life problem be modeled, and what will be the best solution method for the formulated model? Thus, the delivery of fresh fruits in good condition to distant retailers from the production/supply area (depot) is a very challenging task for the wholesaler to obtain a maximum profit while keeping the transportation cost as reasonable as possible and performing the corporate social responsibility (CSR) wrt. environment. Hence, there is a void in the area of delivery systems of perishable products for maximum profit in the context of present-day developed infrastructure and global warming.

To overcome the above lacunae, in this investigation, an attempt is made to answer the above questions in the delivery of fresh fruits by the wholesaler in the minimum possible time to distant retailers from the production/supply area (depot) for maximum profit and keeping the GHGE at a minimum level. Here, the corresponding risk due to driver fatigue against continuous journeys is imprecisely evaluated for each routing plan. This study is significant because it saves the unnecessary wastage of fruits and vegetables (perishable goods). It also reduces the GHGE, the main global warming source. Moreover, it brings maximum possible profit for the wholesaler using the present-day infrastructural facilities and discharging the CSR.

The fireworks algorithm (FWA) (Tan & Zhu, 2010) is one of the most recently developed swarm intelligence algorithms, which imitates fireworks explosions and is used to solve both continuous and discrete (Guendouz et al., 2017) problems. The FWAs can be made more efficient by introducing better stochastic operators and/or using imprecise inferences (Type-1 and Type-2 fuzzy logic) among their parameters, such as sparks and amplitude coefficient. With this objective, here, two discrete FWAs (DFWAs), i.e., DFWA with Type-1 fuzzy logic (T1FLDFWA) and Type-2 fuzzy logic (T2FLDFWA), are developed to solve NP-hard problems. The supremacy of T2FLDFWA is established through a statistical test.

In this investigation, after receiving consignments from producers, the wholesaler/supplier of perishable goods, especially fruits, makes different packages per distant retailers' demands. A vehicle with the required number of fresh items starts from a depot, travels through the appropriate routes following the optimum routing plan, drops the packages at different nodes as per the orders, and returns to the depot (retailer and node are interchangeably used throughout this paper). There are several route connections between the depot and nodes and among the nodes. The demands of the retailers are deterministic and known beforehand. The selling price of the items depends on their freshness, which decreases with time depending on the product. Two different time-dependent freshness expressions are considered. Here, the vehicle speed plays a significant role in determining the delivery times of goods at nodes and the total travel time. The vehicle's speed is also considered in two different ways: in one case, it is an average speed throughout the tour (a decision variable to be determined), and for the other one, it is randomly generated within the route-specific minimum and maximum limits. The vehicle passes through some routes with toll plazas where it spends some time to pay road taxes (termed a fixed charge). The goods are unloaded at the nodes, and some costs and times are spent for this purpose. Fuel cost (FC) is dependent on travel distance, velocity, and weights (curb and commodities). Unit goods transportation cost decreases gradually as the goods' weight increases in the All Unit Discount (AUD) form. In this routing, the vehicle's driver takes 15 min to rest after every 2 h of a continuous journey to release their fatigue. Considering the traveling time, goods transportation cost, fixed carrying cost, unloading cost and time, route-dependent fixed charge and time spent for this, fuel cost, driver's salary and rest, and revenue from the sale, the proposed MrFPGRMs are formulated. The objective is to find the appropriate travel route between the nodes (including the depot), the optimal routing plan, and the vehicle velocity so that the wholesaler can achieve maximum profit, and reduce fuel cost or both.

For the solution, DFWAs based on Type-1 and Type-2 fuzzy logic are developed, of which T2FLDFWA is more efficient. The proposed MrFPGRMs are solved using T2FLDFWA and illustrated numerically. A real-life practical representation of the model is presented for profit maximization. Some managerial decisions are commented on. A trade-off between the model's profit and CE or FC is demonstrated. The results with some risks due to continuous driving are presented.

The key innovations and findings of the present investigation are as follows:

- The present investigation is of twofold: development of (i) new real-life wholesaler fresh produce distribution problems for profit maximization, fuel cost minimization and both freshness and driver fatigue as criteria and (ii) DFWAs using Type-2 fuzzy inferences for the solution of NP-hard problems.
- A multiroute goods delivery system for perishable items to retailers is formulated as a 3D traveling salesman problem (TSP). To date, none have considered fresh produce delivery systems with multiple routes among the nodes and connecting the nodes with the depot.
- Two time-dependent freshness functions (one newly proposed) are considered.
- For the first time, the wholesaler's maximum profit, minimum fuel cost, and both are evaluated, taking the contradiction between freshness (revenue) and the vehicle velocity (transportation cost) into account. A trade-off between profit and fuel cost is presented, which is economically vital for the management.
- Interestingly, minimum fuel cost (maximum greenness) does not confer maximum profit.
- For the first time, in the development of proposed models and their solutions, driver fatigue is taken into account. Against the risk of continuous driving, the increase in profit and sharing it with the driver are discussed.
- For maximum profit and minimum fuel cost, the Pareto front of possible solutions is presented.

- Two imprecise T1FLDFWA and T2FLDFWA are developed using fuzzy inferences and T2FLDFWA is used to solve the proposed MrFPGRMs. T2FLDFWA is a new heuristic algorithm in the literature on swarm optimization that can be applied to other NP-hard problems.
- Some useful managerial decisions are commented on.

The paper is arranged as follows: Sections 1 and 2, give a glimpse of the introduction and motivation and literature review, respectively. Section 3 presents the proposed MrFPGRMs. The solution methodology and proposed solution methods, T1FLDFWA and T2FLDFWA, are described in Section 4. Section 5 is dedicated to efficiency and statistical (analysis of variance (ANOVA)) tests for the T2FLDFWA. Section 6 includes numerical experiments. Parametric analyses are presented in Section 7. Section 8 presents practical implementation and some managerial decisions. The conclusion and future scope are available in Section 9. An Appendix containing type reduction of Type-2 fuzzy is added.

2. Literature review

2.1. TSP-related research

TSP is an age-long problem and has several applications in real-life areas. TSP is practically implemented in vast areas such as transport, network routing, and logistic problems. Lawler (1985) mapped many real-life problems, such as food delivery and container movement, as TSPs. The vehicle routing problem (VRP) is also considered a TSP-type problem. Recently, to solve the TSP in different environments, taking different available vehicles between the nodes as the third dimension, an imprecise multiobjective genetic algorithm (GA) was developed by Maity et al. (2016). Çam and Sezen (2020) presented a linear programming model for passenger bus routing (VRP) and minimized the total idle time. The branch and bound method was used to solve the above model. A variant of TSP, Energy Minimization TSP, was formulated to optimize the total traveling distance and weight of the goods and solved using Christofides's heuristic and Branch and Bound methods (Wang et al., 2020). Krishna et al. (2021) formulated a TSP with traveled distance minimization and solved the model using a hybrid algorithm, which is a combination of the Rider Optimization and Spotted Hyena Optimizer algorithms. A novel approach for hostel selection based on some important attributes related to the modern-day consumer perspective was presented by Kuzmanović and Vukić (2021) using discrete choice analysis.

2.2. Fresh produce-related research

Formulated as TSP, there are several delivery problems of perishable items in the literature. Gokarn and Kuthambalayan (2019) studied the influence of some uncertain parameters such as the supply, demand, and price of fresh produce in the supply chain, survey data collected and fed to a structural equation model (SEM) to validate the formulated model. Cost-saving vehicle scheduling for perishable products was considered by Wang et al. (2017) by maximizing customer satisfaction. A multiobjective programming model for a sustainable supply chain for perishable food products was presented by Jouzdani and Govindan (2021), to optimize total cost, fuel consumption, and traffic congestion. Perishable items related to the inventory routing problem were proposed and solved by Dai et al. (2020) using a hybrid heuristic. A study was conducted on the importance of collaborative resource sharing between transportation and distribution of fresh and perishable products in logistics operations with special infrastructure (e.g., refrigerated trucks/vehicles) (Wang et al., 2021). For the solution of the above model, the authors used a hybrid method combining extended k-means and TS-NSGA-II algorithms. Chen et al. (2018) presented a shipment consolidation problem based on a quantity and quality-dependent policy for a perishable product supply chain by integrating freshness-keeping effort decisions. A fresh fruit (kiwi) transportation problem for e-commerce was formulated and solved using the Floyd algorithm by Gao et al. (2020), taking the maturity of kiwi fruit into account. A multiobjective solid transportation problem for perishable items was formulated under a fuzzy environment and solved by the fuzzy TOPSIS approach, the ϵ-constraint method, and neutrosophic linear programming (Ghosh et al., 2022). Rohmer et al. (2019) formulated a two-echelon inventory routing problem for fresh produce using mixed integer programming to minimize the holding cost and total transportation cost. This model was solved by an adaptive large meta-heuristic neighborhood search. A multipath, multidepot, multiproduct, and multimodal routing problem with total cost minimization as an objective for fresh fruits in an online supermarket was formulated using a mixed-integer programming model (Zhuang et al., 2019). This model is solved by the demand split method. In developing countries such as India, cold transportation is seldom used to transport fresh fruits and vegetables from the wholesaler's air-conditioned depot/storehouse to retailers situated at different locations/nodes. In this system, an attempt is made to reach the retailers as early as possible to preserve the time-dependent freshness of the items, as the selling price to retailers depends on the item's freshness. This venture increases the transport cost along with the consumption of fuel. Thus, a trade-off occurs between the profit and fuel cost. Such a realistic phenomenon is modeled here wrt. profit maximization of the wholesaler and solved using the developed T2FLDFWA.

2.3. Emission-related research

Fuel cost is an important issue in any transportation problem. Barth and Boriboonsomsin (2009) and Scora and Barth (2006) developed comprehensive emission models for fuel consumption and related carbon emissions for heavy-duty diesel vehicles. This comprehensive model is further applied in many VRPs to calculate fuel consumption by Bektaş and Laporte (2011). Poonthalir and Nadarajan (2018) formulated a biobjective fuel-efficient green VRP with varying speed constraints. Here, it is mentioned that varying speed is a more realistic way to represent any TSP-type problem. A multiobjective transportation-p-location problem was formulated by Das and Roy (2019) with the aim of minimizing the carbon emission cost, and total transportation cost and time. To obtain nondominant solutions, a hybrid approach based on an alternating locate-allocate heuristic and neutrosophic compromise programming was used. Mardani et al. (2020) presented a review paper on applying SEM in assessing sustainable and green supply chain management. An eco-friendly VRP was solved by Soon et al. (2019) considering urban congestion. The authors studied traffic congestion's effect and established the emission's relevance. Demir et al. (2014) presented a review of 25 emission models and suggested that the comprehensive emission model is more flexible and reliable for fuel consumption. Giri and Roy (2022) formulated a green 4D transportation problem with fixed charge, carbon emission, transportation cost and time considered as objectives. The above model was solved using neutrosophic programming and Pythagorean hesitant fuzzy programming. According to Micheli and Mantella (2018), the amount of fuel consumption depends on the vehicle type, the velocity of the vehicle, and the weight of the transported goods, including the vehicle's weight. This conjecture has been implemented in the proposed model. A profit maximization model to find the optimal replenishment time and optimal green concern level was designed and solved using Mathematica software (Paul et al., 2022). A green meal delivery routing problem optimizing carbon emission, customer satisfaction, and rider balance utilization was presented and solved with the help of principal component analysis, NSGA II, adaptive large neighborhood search, tabu search, and GA (Liao et al., 2020). Using an iterated local search algorithm and mixed-integer programming, a

two-stage stochastic programming model based on the impact of carbon emissions in the cold supply chain with carbon tax regulation and under uncertain demand was developed to determine optimal replenishment policies and transportation schedules to minimize both operational and emissions costs (Babagolzadeh et al., 2020).

2.4. FWA-related research

Currently, swarm intelligence (SI) has gained enormous popularity among researchers who are working on optimization (Garnier et al., 2007), because SI algorithms possess many advantages for solving various optimization problems. Among various SIs, Kennedy and Eberhart (1995) first published particle swarm optimization (PSO), ant colony optimization (ACO) system was presented by Dorigo et al. (1991), and FWA by Tan and Zhu (2010) in 2010, etc. Kıran et al. (2012) implemented a novel hybrid approach by combining PSO and ACO for estimating the energy demand of Turkey. For solving numerical and constrained engineering optimization problems, Khalilpourazari and Khalilpourazary (2019) proposed a hybrid algorithm combining water cycle and moth-flame algorithms. Altinoz and Yilmaz (2019) implemented the stochastic Newton–Raphson-like step size method-based Hooke–Jeeves algorithm for multiobjective optimization. Due to the method, the algorithm's performance is dependent on the decision space dimension rather than the number of objectives. The FWA is a relatively new SI algorithm in the set of metaheuristic methods and a very efficient algorithm for searching for a near-optimal solution. It is based on the working principle of fireworks. The explosion process is implemented as a searching strategy to find the solution space for an optimal solution by generating sparks around the solution. Classical FWA contains two major components: the number of sparks and the amplitude of the explosion. Originally, FWA was introduced with Gaussian mutation and roulette wheel selection. Later, an improved version of the FWA with the concept of selection, crossover, and mutation operators to enhance information sharing was formulated by Zheng et al. (2015). Very recently, Liu and Qin (2021) studied traffic flow prediction using the FWA. The authors proposed a spark generation mechanism using neighborhood information.

Initially, the FWA was designed for continuous problems (Janecek & Tan, 2011), and later, its discrete version (DFWA) was first proposed by Abdulmajeed and Ayob (2014) using random move and swap operations to generate several solutions. Tan (2015) further developed the DFWA by introducing changes in the explosion operator, selection strategy, and mutation operator in the conventional FWA. As mentioned above, in the FWA, the explosion amplitude depends on the number of sparks. There is a relation between these two parameters. In a real-life situation, it is not possible to count the number of sparks and to measure their amplitudes. These are quantified imprecisely, and relations are represented by fuzzy inferences. The common framework of fuzzy inferences allows the handling of uncertainty in information. A fuzzy set, i.e., a Type-1 fuzzy set, is used to represent the uncertainty by numbers in the range [0, 1]. This imprecise representation of the relation between sparks and the amplitude coefficient is used to obtain the best balance between exploration and exploitation. Again, in Type-1 fuzzy sets, only the degree of achieving the characteristics of the object is determined, whereas in Type-2 fuzzy sets, the above degree of achieving the characteristics is not deterministic; rather, the uncertainty is introduced in the definition of the membership function. In this way, the Type-2 fuzzy set represents impreciseness much better than the Type-1 fuzzy set. Thus, the introduction of Type-1 and Type-2 fuzzy logic (FL) in DFWA gives better algorithms. Moreover, in real-life problems, the dataset representing a variable follows a normal distribution. For this reason, Gaussian Type-1/Type-2 fuzzy membership functions (MFs) are assumed, although other MFs can also be considered.

2.5. Type-1 and type-2 fuzzy logic-related research

A hybrid controller based on Type-1 fuzzy logic (Takagi–Sugeno) was introduced to control the zinc oxide additive rate in a zinc production plant (Xie et al., 2019). Additionally, an interval Type-2 fuzzy logic-based controller was used to control the flow of oxygen. Castillo et al. (2016) presented a comparative study of Type-2 fuzzy logic controller systems against Type-1 and interval Type-2 fuzzy logic controller systems. Using benchmark functions, the superiority of the generalized Type-2 fuzzy controller system was verified. Sun et al. (2015), used an RNA genetic algorithm to optimize the parameters of Type-1 and Type-2 fuzzy logic systems wrt. double inverted pendulum system. Özmen et al. (2017) implemented a robust time-discrete target-environment regulatory system under polyhedral uncertainty through robust optimization. A modified GA with an in vitro fertilization-based selection operator and generation-dependent mutation operator was used to solve the ship routing problem (Das et al., 2021). Here, a triangular fuzzy number was used to treat imprecise cost parameters. Bozanic et al. (2021) developed a multicriteria decision-making method-based neuro-fuzzy system that acts as a decision support system for the selection of construction machines. In the field of FWA, Barraza et al. (2016) used fuzzy logic to adjust FWA parameters and transformed these parameters into dynamic parameters to optimize the performance of the FWA. Another investigation on the performance improvement of FWA was presented by Barraza et al. (2017). They used Type-1 fuzzy logic-based inferences between the number of sparks and explosion amplitude for performance enhancement of FWA. Recently, Type-2 fuzzy logic has been used in different problems (Jovanović & Teodorović, 2022; Ontiveros-Robles et al., 2021; Sanchez et al., 2015). To date, no studies have implemented Type-2 fuzzy inferences in DFWA.

2.6. Research gap

From the above literature survey, it is observed that the investigated fresh fruit delivery systems are two-dimensional (2D). The fruits are transported from the depot to retailers by a single vehicle through a route. With infrastructural developments throughout the world, there are several connecting routes between the different places. None considered this infrastructural change, i.e., the 3D fresh fruit distribution model. There are several freshness functions (of time) in the literature. In reality, fruits/vegetables lose freshness slowly, but after some time, they degrade quickly. There is no appropriate freshness function in the literature to represent this phenomenon. For a long journey, car accidents are frequent due to driver fatigue. There is a risk related to continuous driving, and the driver should rest for 15 min for every 2-h of the ongoing journey (Tucker et al., 2003; Wang & Pei, 2014). None considered these criteria in routing problems. There are many investigations on carbon emissions due to transportation/routing. Profit and CE (fuel cost) behave in opposite directions wrt. each other. None demonstrated this trade-off between profit and fuel cost. Moreover, there are many heuristic methods available for the solution of NP-hard problems such as routing and the traveling purchaser problem (TPP). Very few have used the comparatively new heuristic method, DFWAs. For a better balance between exploration and exploitation, none have used Type-2 fuzzy logic in DFWAs. These research gaps have been removed in the present investigation.

3. Multiroute fresh produce Green routing models (MrFPGRMs)

3.1. Nomenclature

Table 1 presents the notations and descriptions of a few essential parameters used in formulating the proposed MrFPGRMs.

Table 1
Notations and descriptions of parameters and decision variables.

Notations	Description
Node $(1, 2, \ldots, M+1)$	1 indicates depot; $2, \ldots, M+1$ indicates retailers/(nodes)
R	Number of routes
i, j, r, h, k, q	Indices
K	Number of items
T_j	Time to depart from jth retailer.
$H_q^k(T_j)$	Freshness functions of kth item, $q = 1, 2$
D_s	Diver's salary per hour ($)
L	Fuel cost per liter ($)
μ	Curb weight (kg)
V_c	Vehicle capacity (kg)
Ω^k	Sensitive parameter for the freshness of kth product
C_{ijr}^0	Route dependent fixed carrying cost for ith to jth node via rth route ($)
W_i^k	Remaining amount of kth product after visiting ith node (kg)
P^k	Purchasing cost per unit of kth type of product ($)
C_{ijr}^k	Discrete carrying cost for kth item per unit distance per unit weight from ith to jth node via rth route ($)
B_{ijr}^{kh}	Fixed transportation cost per unit distance per unit weight for ith to jth node through rth route within the weight interval $W_{h-1}^k \le W_i^k < W_h^k$ ($)
S^k	Selling price per unit of kth product ($)
tim^k	Self-life of kth product (h)
ϑ_1	Lower limit of travel speed (km/h)
ϑ_2	Upper limit of travel speed (km/h)
A^k	Total amount to be delivered of kth product (kg)
T'_{11}	Total time for the travel — starting from node 1 (depot), visiting all other nodes and then coming back (h)
d_j^k	Demand of kth product at jth retailer (kg)
t^k	Per unit unloading time of kth product at all nodes (h)
dis_{ijr}	Distance from ith to jth node via rth route (km)
t'_{ijr}	Time (fixed) spent at toll plaza to pay taxes on the rth route to travel from ith to jth node (h)
f_{ijr}	Fixed charge paid at toll plaza from ith to jth node via rth route ($)
t''_{ijr}	Driver rest time in between ith node to jth node through rth route (h)
α^k	Per unit unloading cost of kth product at all nodes ($)
	Decision variables
v_{ijr}	Speed of the vehicle from ith to jth node through rth route (km/h)
x_{ijr}	= 1, if vehicle goes from ith to jth node via rth route, otherwise = 0

Vehicle independent parameters		Vehicle dependent parameters	
ξ	Fuel-to-air mass ratio	K_e	Engine friction factor (kJ/rev/l)
g	Gravitational constant (m/s^2)	N_e	Engine speed (rev/s)
ρ	Air density (kg/m^3)	V_e	Engine displacement (l)
τ	Acceleration (m/s^2)	F_a	Frontal surface area (m^2)
c_r	Coefficient of rolling resistance	c_d	Coefficient of aerodynamic drag
ω	Efficiency parameters for diesel engines	ε	Vehicle drive train efficiency
κ	Heating value of a typical diesel fuel (kJ/g)		
ψ	Conversion factor (g/l)		
ϕ	Road angle		

3.2. Multiroute fresh produce green routing models for profit maximization (MrFPGRMsfPM)

3.2.1. Statement of MrFPGRMsfPM

A vehicle with fresh goods is dispatched from a depot and comes back to it after dropping the goods at the retailers' locations (nodes) as per their demands placed in advance. The initial amount of goods is equal to the total retailers' demands. There are several routes between the depot and retailers and among the retailers. The goods vehicle follows the retailers' appropriate routes and optimum routing plan. The freshness of the goods decreases with time, and the unit selling price depends on the current goods' freshness. The driver takes 15 min to rest after every two hours of a continuous journey.

The multiroute fresh goods delivery problem is represented as a combination of revenue, purchasing cost, goods carrying cost (fixed and variable), unloading cost, fixed charge, driver salary, and fuel cost. The selling price of an item depends on its freshness, which varies with the time gap between its loading and delivery. Thus, the freshness of the goods depends on transportation time, including the driver's rest time, unloading time, and toll payment time. Revenue depends on the freshness of the products. The unloading cost varies with the amount of the product. A fixed charge is associated with different routes and comprises toll taxes, festival subscriptions, and some forced collections. Fuel cost combines the engine module, speed module, and weight module (Micheli & Mantella, 2018). Total travel time is mainly dependent on the vehicle speed (decision variable) and the entire travel distance (route) for routing, which is selected by x_{ijr} (decision variable). Here, the objective is to find the appropriate routes between nodes (optimum routing plan (x_{ijr})) and vehicle's optimum velocity (v_{ijr}) so that the wholesalers can achieve maximum profit or fuel cost is minimum or both.

Let us illustrate a routing problem with ten nodes, of which node 1 is the depot, and nodes $2, 3, \ldots, 10$ are retailers. A truck starts from the depot with two fruit items (1 and 2) and moves to nine different retailers (nodes) to deliver the required number of fruits per the retailers' orders. Here, three different routes $(1, 2, 3)$ are considered between the nodes and denoted by curved lines in Fig. 1.

3.2.2. Mathematical formulation of MrFPGRMsfPM

Following the representation of 3D multiobjective TSP (Maity et al., 2016), the mathematical formulation of the model described in Section 3.2.1 is as follows:

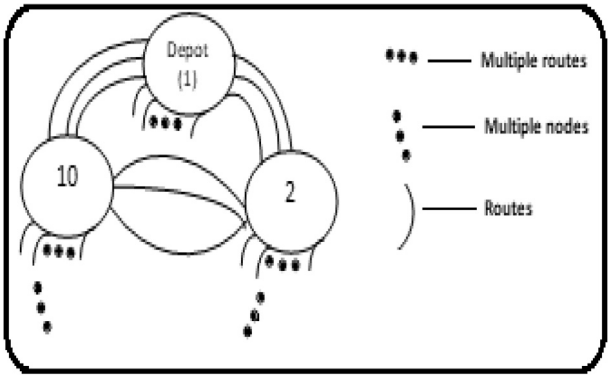

Fig. 1. Block diagram of available routes.

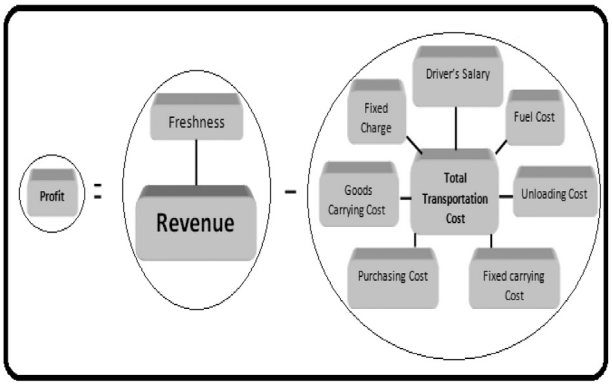

Fig. 2. Block diagram of Model-1.

Maximize Profit = Revenue − (Purchasing Cost + Goods Carrying Cost + Fixed Charge + Driver's Salary + Fuel Cost + Unloading Cost + Fixed Carrying Cost)

(Pictorial representation of the proposed model is given in Fig. 2 for better clarification)

$$\begin{aligned}\text{Max } Z(x_{ijr}, v_{ijr}) = &\underbrace{\sum_{i=1}^{M+1}\sum_{j=2}^{M+1}\sum_{r=1}^{R}\sum_{k=1}^{K}\{S^k H_q^k(T_j)\}d_j^k x_{ijr}}_{Revenue} - (\underbrace{\sum_{k=1}^{K} P^k A^k}_{Purchasing\ Cost} \\ &+ \underbrace{\sum_{i=1}^{M+1}\sum_{j=2}^{M+1}\sum_{r=1}^{R}\{C_{ijr}^0 + \sum_{k=1}^{K} C_{ijr}^k W_i^k dis_{ijr}\}x_{ijr} + \sum_{r=1}^{R} C_{(M+1)1r}^0 x_{(M+1)1r}}_{Total\ Goods\ Carrying\ Cost} \\ &+ \underbrace{\sum_{j=2}^{M+1}\sum_{k=1}^{K} d_j^k \alpha^k}_{Unloading\ Cost} + \underbrace{\sum_{i=1}^{M+1}\sum_{j=2}^{M+1}\sum_{r=1}^{R} f_{ijr}x_{ijr} + \sum_{r=1}^{R} f_{(M+1)1r}x_{(M+1)1r}}_{Total\ Fixed\ Charge} \\ &+ \underbrace{FC}_{Fuel\ Cost} + \underbrace{D_s T_{11}'}_{Driver's\ Salary}),\end{aligned} \tag{1}$$

$$\begin{aligned}FC = &\sum_{i=1}^{M+1}\sum_{j=2}^{M+1}\sum_{r=1}^{R} L\lambda\{y(\frac{dis_{ijr}}{v_{ijr}}) + \gamma\beta dis_{ijr}v_{ijr}^2 + \gamma s(\mu + \sum_{k=1}^{K} W_i^k) dis_{ijr}\}x_{ijr} \\ &+ \sum_{r=1}^{R} L\lambda\{y(\frac{dis_{(M+1)1r}}{v_{(M+1)1r}}) + \gamma\beta dis_{(M+1)1r}v_{(M+1)1r}^2 + \gamma s\mu dis_{(M+1)1r}\} \\ &\times x_{(M+1)1r},\end{aligned} \tag{2}$$

$$W_i^k = (A^k - \sum_{t=2}^{i} d_t^k), \qquad \forall i, k, \tag{3}$$

subject to

$$A^k = \sum_{j=2}^{M+1} d_j^k, \qquad k = 1, 2, \ldots, K, \tag{4}$$

$$\sum_{k=1}^{K} A^k \le V_c, \tag{5}$$

$$\sum_{r=1}^{R} x_{ijr i\neq j} = 1 = \sum_{r=1}^{R} x_{jir j\neq i}, \qquad \forall i, j, \tag{6}$$

$$x_{ijr i\neq j} = x_{jir j\neq i}, \qquad \forall i, j, r, \tag{7}$$

where $i \neq j$, $i = 1, 2, \ldots, M+1$, $j = 2, \ldots, M+1$, $r = 1, 2, \ldots, R$, $k = 1, 2, \ldots, K$, $q = 1, 2$.

Here, $x_{ijr} \in \{0, 1\}$ and $v_{ijr} \in \{\vartheta_1, \ \vartheta_2\}$ are decision variables, and $(\vartheta_1, \vartheta_2) \in R^+$. Fuel consumption related parameters such as vehicle independent terms are calculated as $\lambda = \xi/(\kappa\psi)$, $s = \tau + g sin\phi + g c_r cos\phi$, and vehicle dependent parameters are calculated as $\gamma = 1/(1000\omega\varepsilon)$, $y = K_e N_e V_e$ and $\beta = 0.5 c_d \rho F_a$.

The objective function in Eq. (1) has seven terms. Its 1st term gives the total revenue earned. Here, the unit selling price is dependent on freshness which decreases with time (T_j). The total purchasing cost of items is represented by the 2nd term. The 3rd term furnishes the total goods carrying cost from depot to retailers (nodes) and back to it, which consists of three sub-terms: the first one gives the total fixed carrying cost from depot to the last node, total goods carrying cost from depot to the last node is represented by the second sub-term, and third sub-term is for fixed carrying cost from the last node to the depot. Next, the 4th term represents the total unloading cost of items at different nodes. A total fixed charge (paid by the wholesaler due to travel through different routes) is given by the 5th term. It has two sub-terms: the first subterm is for the total fixed charge paid during the journey from the depot to the last node, and the total fixed charge paid in the return journey from the last node to the depot is represented by the second subterm. The 6th term provides the total fuel cost for the whole journey, and the 7th term calculates the total driver's salary ($D_s T_{11}'$).

Eq. (2) calculates total fuel cost, comprising two sub-terms for onward and backward journey to and from the depot, respectively. Eq. (3) determines the remaining amount of kth item after visiting ith node. The constraint in Eq. (4) satisfies total demand (A^k) for each product. Constraint in Eq. (5) is for the condition that the total demand of the items must be less or equal to the capacity of the vehicle. The constraint in Eq. (6) indicates that the only one route is selected for travel between any two nodes. The symmetry of forward and backward journey is presented by the constraint in Eq. (7).

Total transportation time comprises of three types of time consumption such as travel time (T_j), which depends on the distance (dis_{ijr}) and vehicle speed (v_{ijr}), unloading time (t^k), time spent at toll offices (t'_{ijr}) and driver rest time (t''_{ijr}). It is given by

$$T_j = T_i + \frac{dis_{ijr}}{v_{ijr}} + \sum_{l=1}^{K} d_j^l t^l + t'_{ijr} + t''_{ijr}, \qquad \forall i, j, r, k, \tag{8}$$

where $T_1 = 0$, $T_{11}' = T_{M+1} + \sum_{r=1}^{R}(\frac{dis_{(M+1)1r}}{v_{(M+1)1r}} + t'_{(M+1)1r} + t''_{(M+1)1r})x_{(M+1)1r}$.

Goods carrying cost (C_{ijr}^k) per unit item varies with the weight of materials, and it is of AUD type. Unit goods carrying cost decreases

with the increase of goods' weight and is represented as

$$C_{ijr}^{k} = \begin{cases} B_{ijr}^{k1}, & 0 < W_i^k < W_1^k \\ B_{ijr}^{k2}, & W_1^k \le W_i^k < W_2^k \\ \vdots & \vdots \\ B_{ijr}^{kh-1}, & W_{h-2}^k \le W_i^k < W_{h-1}^k \\ B_{ijr}^{kh}, & W_{h-1}^k \le W_i^k < W_h^k, \end{cases} \tag{9}$$

where $B_{ijr}^{k1} > B_{ijr}^{k2} > \cdots > B_{ijr}^{kh}$, $W_1^k < W_2^k < \cdots < W_{h-1}^k$, $\forall i, j, r, k$.

3.2.3. Representation of freshness

Freshness (color and texture) of fresh produce decreases with time and is counted here from the instant of commencement of the goods vehicle journey, although fruits' freshness decreases from the instant of harvesting. In the case of some fruits, at the beginning, they lose their color and texture slowly, and after a certain time, their rot increases very fast. Taking this real-life phenomenon into account, two types of freshness functions $H_q^k(T_j)$, $q = 1, 2$ are considered. A new exponential decaying freshness function for kth item i.e., $e^{-\Omega^k T_j^2}$ $(= H_1^k(T_j))$ is considered (H_1 in Fig. 3) in this investigation. In this case, after a particular time, its rot increases very fast. Another freshness function $2 - e^{(ln2/tim^k)T_j}$ $(= H_2^k(T_j))$ proposed by Wang et al. (2017), is also used for investigation purpose (H_2 in Fig. 3). It is observed that the newly introduced function $H_1^k(T_j)$ behaves more realistically with the assumptions made on freshness (slow rot at the beginning and then fast).

3.3. Different mrfpgrms

Model-1: MrFPGRMfPM with $H_1^k(T_j)$ and an optimum average vehicle speed

For this Model, the mathematical formulation is given in Section 3.2.2 with $H_1^k(T_j)$ as freshness function and v_{ijr} is the average velocity (AV) (within a given interval) for the whole tour. v_{ijr} is randomly generated within lower and upper limits (ϑ_1, ϑ_2) for every candidate solution i.e., routing plan. Maximum profit is determined by using the optimum routing plan for the whole tour and appropriate routes between the nodes obtained through optimization of Eq. (1).

Model-2: MrFPGRMfPM with $H_1^k(T_j)$ and a route-dependent velocity (RDV)

Following Poonthalir and Nadarajan (2018), minimum and maximum speed limits (a, d) for every route are considered, and the possible average speed on that route is generated using trapezoidal distribution within the vehicle's speed limits. v_{ijr} in Eqs. (1) and (2) is determined by taking a speed for each route following trapezoidal distribution (Fig. 4).

The trapezoidal distribution density function is given in Eq. (10)

$$f(x|a,b,c,d) = \begin{cases} 0, & x < a \\ u\left(\frac{x-a}{b-a}\right), & a \le x < b \\ u, & b \le x < c \\ u\left(\frac{d-x}{d-c}\right), & c \le x < d, \end{cases} \tag{10}$$

where $a \le b \le c \le d$, $u = \frac{2}{d+c-b-a}$, a and d being minimum and maximum speed limits respectively.

Expectation of the probability density function (PDF) in Eq. (11) is

$$E(x) = \int_a^b u\left(\frac{x-a}{b-a}\right)x\,dx + \int_b^c ux\,dx + \int_c^d u\left(\frac{d-x}{d-c}\right)x\,dx. \tag{11}$$

Model-3: MrFPGRMfPM with $H_2^k(T_j)$ and an optimum average vehicle speed

It is same as Model-1 with $H_2^k(T_j)$ in the place of $H_1^k(T_j)$.

Model-4: MrFPGRMfPM with $H_2^k(T_j)$ and a route-dependent velocity (RDV)

This model is same as Model-2 with $H_2^k(T_j)$ instead of $H_1^k(T_j)$.

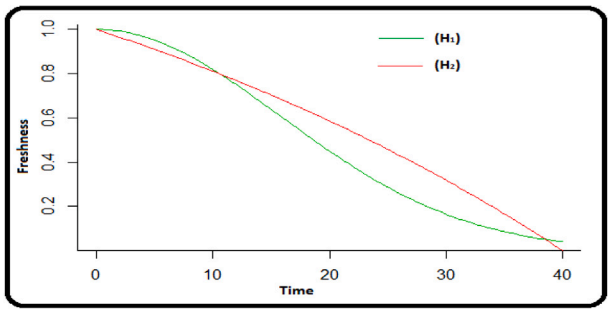

Fig. 3. Graphical representation of freshness functions.

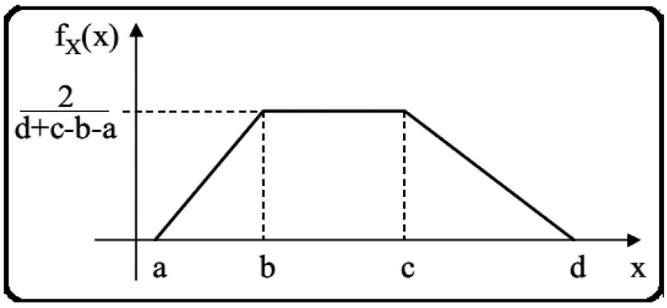

Fig. 4. PDF of trapezoidal distribution.

The mathematical formulations of Models-3 and 4 are same as the Models-1 and 2, respectively.

Model-5: Multiroute Fresh Produce Green Delivery Model for Fuel Cost Minimization (MrFPGRMfFCM)

Here, fuel cost is minimized and implemented as Min FC (given by Eq. (2)) with $H_1^k(T_j)$ and Model-1's parameters.

Model-6: Multiroute Fresh Produce Green Delivery Model for both Profit Maximization and Fuel Cost Minimization (MrFPGRMfPMFCM)

It is a multiobjective optimization model combining both MrFPGRMfPM and MrFPGRMfFCM. Here, both profit and fuel cost are respectively maximized and minimized. It is implemented with $H_1^k(T_j)$ and Model-1's parameters. The multiobjective is converted to a single objective using L_p−metrics method (Branke et al., 2008) considering $p = 1$. Taking optimum profit with corresponding fuel cost from Model-1 and optimum fuel cost along with corresponding profit from Model-5, payoff matrix is prepared. Then L_p−metrics is formulated as

$$\text{Min } \Theta = \varpi \frac{Fuel - Fuel^*}{Fuel^+} + (1-\varpi)\frac{Profit^* - Profit}{Profit^*}, \tag{12}$$

where $Fuel^*$ and $Profit^*$ are optimum fuel cost from Model-5 and optimum profit from Model-1, respectively. ϖ is the weight given to the objectives, $Fuel^+$ is the corresponding fuel cost for optimum profit from Model-1, $Fuel$ and $Profit$ are the objectives.

The model classifications are given in Fig. 5.

4. Solution methodology: Development of T1FLDFWA and T2FLDFWA

In this investigation, two new DFWAs incorporating Type-1 and Type-2 fuzzy logic (T1FLDFWA and T2FLDFWA, respectively) are developed for optimization.

4.1. Existing discrete fireworks algorithm (DFWA)

Inspired by the explosion of fireworks, the FWA was developed, and it is very efficient for solving global optimization problems (Tan

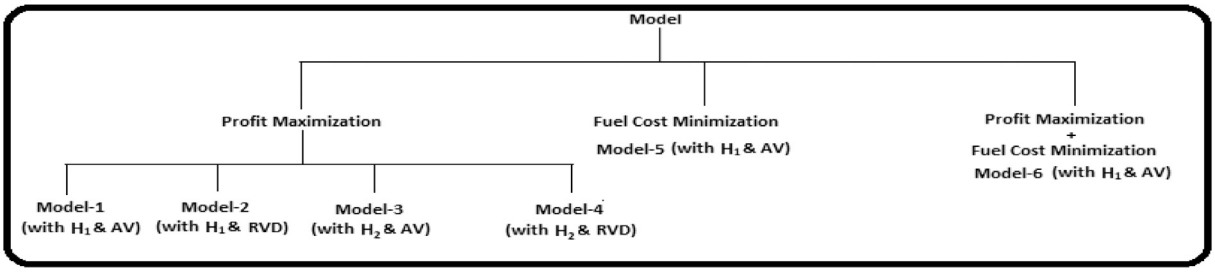

Fig. 5. Block diagram of models.

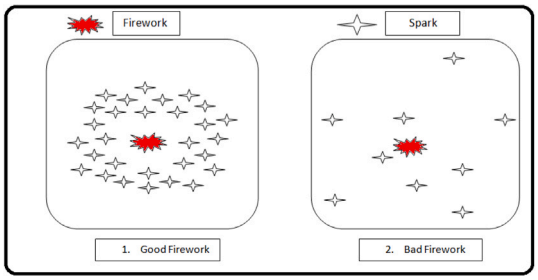

Fig. 6. Fireworks explosion.

& Zhu, 2010). Here, in the DFWA, a few fireworks (locations) are selected randomly as initial individuals in the potential search space. Then, their corresponding fitness is evaluated. For every explosion, the corresponding parameters such as the number of sparks and amplitude of the explosion, are calculated. The Gaussian mutation operator is used to mutate some sparks. Selection of an equal number of fireworks for the next generation from the set consisting of all newly generated sparks and original fireworks is made using a distance-based selection operator. DFWA stops after a predefined number of iterations or when the required accuracy is found. The whole idea is presented mathematically in the following steps.

4.1.1. Initialization

Some random one-dimensional vectors (with nonrepeated nodes) are selected from the solution space, which are used as initial solutions for the first generation. Number of fireworks is denoted as N, and $X_\varkappa$ represents the $\varkappa$th firework.

4.1.2. Spark generation

a. Calculation of the number of sparks and amplitude of the explosion

Bad fireworks are characterized by a small number of sparks with high amplitude. On the other hand, good fireworks have a large number of sparks with small amplitudes. Bad fireworks are responsible for global search (exploration), and good fireworks are responsible for local search (exploitation). The actual power of this algorithm comes from a better balance between exploration and exploitation, i.e., a balance between the number of good and bad fireworks. The following Fig. 6 illustrates the different fireworks.

Let $\Gamma_\varkappa$ and $\Theta_\varkappa$ represent respectively the number of sparks and explosion amplitude of corresponding firework $X_\varkappa$.

$$\Gamma_\varkappa = \eta \times \frac{G_{max} - G(X_\varkappa) + \Delta}{\sum_{\varkappa=1}^{N} (G_{max} - G(X_\varkappa)) + \Delta}, \tag{13}$$

where $G_{max} = max(G(X_\varkappa))$, $\varkappa = 1, 2, 3, \ldots, N$, $G(X_\varkappa)$ is the corresponding fitness of $X_\varkappa$, and η is a parameter that controls the total number of sparks generated by a firework, and Δ is a very small machine-dependent positive constant for avoiding error occurred due to division by zero. The above equation yields a real value of $\Gamma_\varkappa$, but the number of sparks must be a positive integer. Therefore, the real value is converted into the whole number as follows (Eq. (14)):

$$\Gamma_\varkappa = \begin{cases} round(a1 \times \eta), & \Gamma_\varkappa < a1 \times \eta \\ round(b1 \times \eta), & \Gamma_\varkappa > b1 \times \eta \\ round(\Gamma_\varkappa), & \text{otherwise,} \end{cases} \tag{14}$$

where $a1$ and $b1$ are constants and $a1 < b1 < 1$.

Mathematically, amplitude of the explosion is defined as:

$$\Theta_\varkappa = A_m \times \frac{G(X_\varkappa) - G_{min} + \Delta}{\sum_{\varkappa=1}^{N} (G(X_\varkappa) - G_{min}) + \Delta}, \tag{15}$$

where $G_{min} = \min(G(X_\varkappa))$, $\varkappa = 1, 2, 3, \ldots, N$, A_m denotes the maximum explosion amplitude.

b. Generating explosion spark

The $\varkappa$th firework generates $\Gamma_\varkappa$ number of sparks using Eq. (13) in a hyper sphere having radius as $\Theta_\varkappa$. The sparks are generated randomly in different dimensions (P) using Eq. (16). Actually a spark $\vec{X}_\zeta$ generated by the firework $X_\varkappa$ (selecting p dimensions of $X_\varkappa$, $p \in P$), is calculated by Eq. (17). The Eqs. (16) and (17) are as follow:

$$P = round(D * rand(0, 1)), \tag{16}$$

where D is the dimension of $X_\varkappa$ and $P < D$.
Now for each dimension p,

$$\vec{X}_\zeta^p = X_\varkappa^p + \Theta_\varkappa \times rand(0, 1), \tag{17}$$

where $\varkappa = 1, 2, \ldots, N$, $\zeta = 1, 2, \ldots, \Gamma_\varkappa$.

To restrict the value of $\vec{X}_\zeta^p$ within the search space of the problem, a mapping operator in Eq. (19), which is described in Section 4.1.2.d, is used. For a discrete version of FWA, generated sparks should be a combination of non-repeated nodes.

c. Generating Gaussian spark

Additionally, to maintain spark diversity (mutation), a Gaussian distribution is used. A few fireworks are selected and changed using the following equation:

$$\hat{X}_\varkappa^p = X_\varkappa^p \times Gaussian(1, 1). \tag{18}$$

d. Mapping operator

Sparks generated from the above two procedures (Sections 4.1.2.b, and 4.1.2.c) can be out of bound of feasible space. Then a mapping operation is used (every spark is a one-dimensional vector with non-repeated nodes). The mathematical formulation of the operator is as follows:

$$\bar{X}_\varkappa^p = X_{min}^p + |X_\varkappa^p| \%(X_{max}^p - X_{min}^p), \tag{19}$$

where X_{min}^p, X_{max}^p stand for the maximum and minimum boundaries of corresponding spark position respectively.

4.1.3. Selection of location

The best firework in the current generation always goes to the next generation, and the rest of the fireworks are selected based on probability proportional to their distance from others.

4.2. Proposed Type-1 and Type-2 fuzzy logic-based discrete fireworks algorithms (T1FLDFWA and T2FLDFWA)

The conventional FWA has some performance-related issues that can be solved to enhance the performance while keeping the basic principle unchanged. In the proposed T1FLDFWA and T2FLDFWA, a new mutation process named square mutation, which is generation-dependent rather than Gaussian mutation (deterministic), is implemented. A new selection method, probabilistic selection instead of roulette wheel (RW) selection, is employed. Both techniques are discussed as follows:

Generation dependent probability of mutation p_m is calculated as

$$p_m = \frac{Q}{g_n^2}, Q \in [0, 1], \tag{20}$$

where g_n is current generation number.

The process of mutation depends on whether a randomly generated number $r1$ within $[0, 1]$ is less than the probability of mutation p_m and it decreases with an increase in generation. Algorithm 1 depicts the whole process.

Probabilistic selection helps in fast convergence in contrast to RW selection. The value of the probability of the selection operator (p_s) is predefined. For the selection of fireworks, the same condition is checked again $r2 < p_s$, where $r2$ is a random number within $[0, 1]$.

Boltzmann-Probability (p_B) is used to choose those solutions which are closer to optimum fitness solution for better convergence. Here, $p_B = e^{(G(X_\varkappa)-G_{max}/\Lambda)}$, $\Lambda = \Lambda_0(1-\iota)^\varrho$, $\varrho = (1 + 200 * (g_n/M_g))$, where g_n indicates current generation number, M_g for maximum generation number, $\Lambda_0 = rand[25, 250]$, $\iota = rand[0, 1]$, $G(X_\varkappa)$ is the fitness function of firework $X_\varkappa$.

A fuzzy inference system is introduced based on linguistic variables, which depend on the membership function. One input variable is sparks (number of sparks), and one output variable is the amplitude coefficient (explosion amplitude). This fuzzy system contains (i) Mamdani Type, (ii) sparks as an input variable, (iii) amplitude coefficient as the output variable, and (iv) centroid defuzzification method, which is described in the Appendix.

4.2.1. Flowchart for fuzzy logic based-DFWA

The flowchart of fuzzy logic-based DFWA is presented in Fig. 7. T2FLDFWA algorithm is given in Algorithm 2 for better representation.

4.2.2. Rules for Type-1 and Type-2 fuzzy logic

For controlling the Amplitude coefficient, the 3 rules (Fig. 8) and the corresponding fuzzy linguistic values (Tables 2 and 3) are used.

4.2.3. Parameter settings for the algorithm

Here, Table 4 contains the values of the parameters used in the T1FLDFWA and T2FLDFWA.

4.2.4. Fuzzy linguistics input/output values

The linguistic values are presented in Tables 2 and 3 for sparks and Amplitude coefficient, respectively.

4.2.5. Amplitude coefficient by Type-1 fuzzy logic

Using the rules (Fig. 8) and linguistic values (Tables 2 and 3), the amplitude coefficients are evaluated and presented in Figs. 9(a) and 9(b). Here, using the rule-3 for Type-1 fuzzy logic, it is observed that in a certain scenario, the amplitude coefficient is 22.5 when the number of sparks is 10.

Table 2
Fuzzy input.

	Sparks
Few	[6.5 −02.5 02.5]
Some	[6.5 16.5 20.5]
Enough	[4.5 36.5 40.5]

Table 3
Fuzzy output.

	Amplitude coefficient
Small	[−1.5 6 13 1.5 9 16]
Medium	[12 21 29 16 24 31]
Big	[29 34 45 31 38 45]

Table 4
Parameters setting for methodology.

Parameters	Values
Number of Fireworks (N)	10
Maximum number of Sparks for each firework	40
Control Parameter (η)	45
Constants (a1 and b1)	0.03 and 0.85
Maximum explosion amplitude (A_m)	42
Probability of mutation (p_m)	0.1
Maximum number of evaluations/generation (M_g)	5000
Input variable (sparks)	[1, 40]
Output variable (Amplitude coefficient)	[0, 45]

4.2.6. Amplitude coefficient by Type-2 fuzzy logic

Using Type-2 fuzzy logic, the amplitude coefficients based on the inference rules (Fig. 8) and linguistic values (Tables 2 and 3) are evaluated and presented in Fig. 9.

The amplitude coefficient is more dynamic (Figs. 9(c) and 9(d)) compared to Type-1 fuzzy logic for the same set of rules (Figs. 9(a) and 9(b)). On the other side, Figs. 9(e) and 9(f) indicate Spark's membership and interval rule viewer for Type-2 fuzzy logic, respectively.

The proposed Algorithms T1FLDFWA and T2FLDFWA with generation-dependent square mutation and probabilistic selection dynamically use Type-1 and Type-2 Fuzzy Logic tools to produce the amplitude coefficient for given sparks.

Algorithm 1 Generation dependent square mutation

1: Calculate g_n^2, g_n = current generation number
2: Calculate $p_m = \frac{Q}{g_n^2}$, $Q \in (0, 1)$
3: for each firework in the population do
4: Randomly generate $r1 = rand(0, 1)$
5: if $r1 < p_m$ then
select current firework (X)
6: $a2 = rand[2, M + 1]$
7: $b2 = rand[2, M + 1]$
8: if $a2 = b2$ then
goto step 6
9: for every nodes in the route do
10: if $X[n] = a2$ then
$p1 = n$
11: else if $X[n] = b2$ then
$q1 = n$ // $p1, q1 \in [2, M + 1]$
12: $X[p1] = b2$, $X[q1] = a2$ // replace a2 by b2 and b2 by a2.
13: end for
14: end if
15: end for

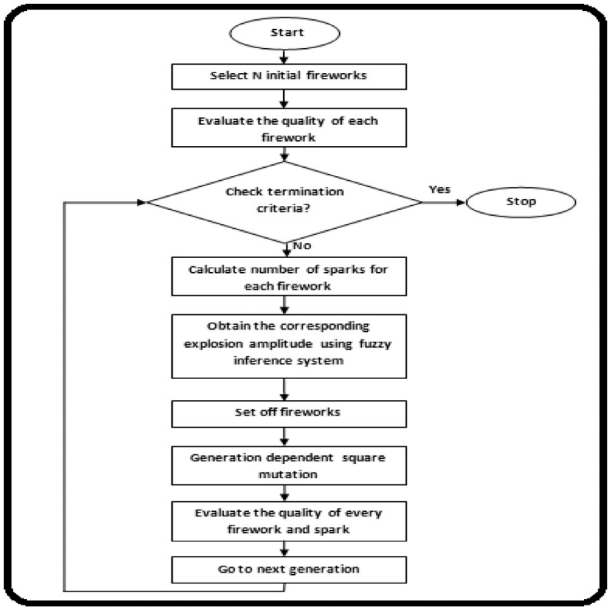

Fig. 7. Flowchart for fuzzy logic based-DFWA.

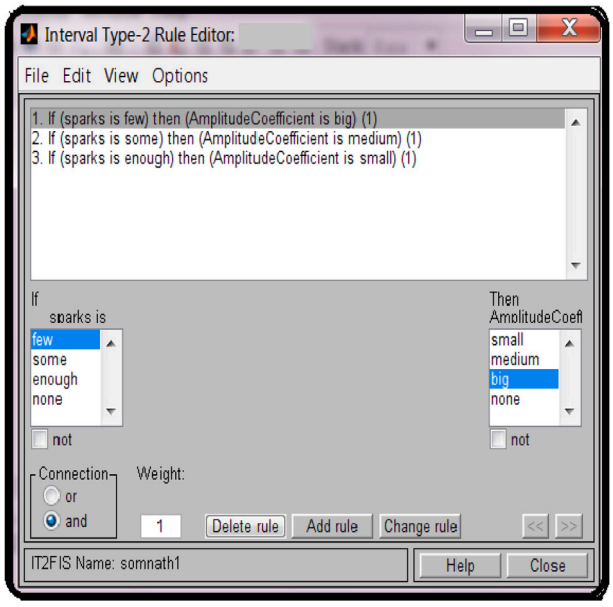

Fig. 8. Inference rules for Type-1 and Type-2 fuzzy logic.

Algorithm 2 T2FLDFWA

1: Generate N initial locations (fireworks)
2: Calculate fitness function $G(X_\varkappa)$ for each firework, $\varkappa = 1, 2, \cdots, N$
3: while (termination criteria)
4: Set off N fireworks
5: for each firework $X_\varkappa \in N$ do
6: Calculate the number of sparks ($\Gamma_\varkappa$) for each firework $X_\varkappa$ using Eq. (13)
7: Calculate Amplitude coefficient ($\Theta_\varkappa$) each firework $X_\varkappa$ using Type-2 fuzzy logic inference rule described in Section 4.2.2
8: Calculate P (direction) for each fireworks $X_\varkappa$ using Eq. (16)
9: end for
10: for $\varkappa = 1 : m$ do // m is number of iteration per generation
11: Randomly select few fireworks depending upon p_m and mutate them using Algorithm 1
12: Evaluate the quality of newly created sparks
13: end for
14: Select N best fitted candidates from the set of sparks and fireworks using the probabilistic selection as given in Section 4.2
15: end while
16: Return the best fireworks

5. Efficiency tests for T2FLDFWA

In this section, it is established that out of the two methods T1FLDFWA and T2FLDFWA, the latter gives better results.

5.1. Results of T1FLDFWA and T2FLDFWA against some benchmark instances

The performance of the proposed T1FLDFWA and T2FLDFWA is established by solving 12 standard benchmark problems from TSPLIB, whose results are given in Table 5. By comparing all the problems in terms of the total cost, the number of iterations, and the CPU time, the results are obtained for 25 independent runs.

Table 5
Results of standard TSP Problem (TSPLIB)

Instances	BKS	T2FLDFWA			T1FLDFWA		
		BFS	Iteration	Time (s)	BFS	Iteration	Time (s)
burma14	3323	3323	144	0.39	3323	158	0.67
gr17	2085	2085	173	0.58	2085	193	0.93
gr24	1272	1272	186	0.89	1272	223	1.19
bayg29	1610	1610	198	1.12	1610	257	1.39
dantzig42	699	699	237	1.52	699	287	2.26
swiss42	1273	1273	259	1.96	1273	315	2.91
hk48	11 461	11 461	285	2.57	11 523	364	3.26
brazil58	25 395	25 395	416	3.14	26 870	498	4.12
eil76	538	538	623	5.14	538	567	6.25
gr96	55 209	55 714	746	6.25	57 814	817	8.03
kroE100	22 068	24 187	817	7.47	27 496	928	9.14
eil101	629	674	873	5.28	679	1086	6.17

BKS: Best-known solution, BFS: Best found solution.

5.2. Statistical test

A statistical test, ANOVA, is performed using 10 benchmark instances from Table 5. Three different algorithms, T2FLDFWA, T1FLDFWA, and GA (with RW selection, cyclic crossover, and random mutation), are chosen to compare the efficiency. Table 6 presents the number of achievements in 100 individual runs for the given benchmark instances using the Algorithms T2FLDFWA, T1FLDFWA, and GA, separately.

An equal number of benchmark instances ($I = 10$) is taken for each algorithm ($J = 3$). The sample means are $\overline{X_1} = 81.1$, $\overline{X_2} = 71.5$, $\overline{X_3} = 62.9$.

The critical value of F is $F_{0.05(2,27)} \approx 3.32$. As the computed F (in Table 7) is higher (29.6714) than the critical F value (3.32) for a 0.05 level of significance, it could be concluded that a striking contrast exists between the groups. When the F ratio is significant in an ANOVA with more than two groups, it should be followed by multiple comparison tests to determine which group's mean is significant in comparison

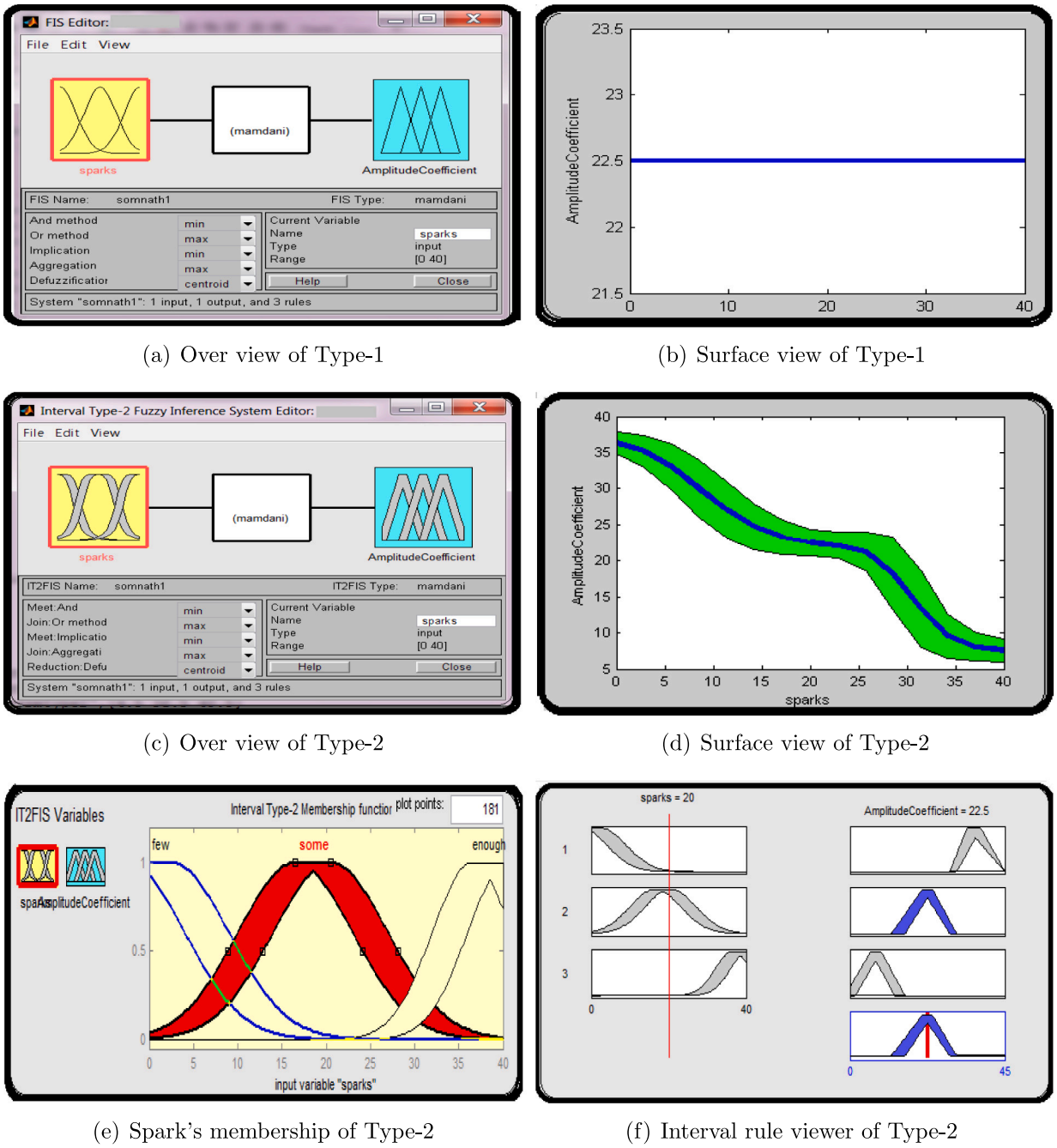

(a) Over view of Type-1

(b) Surface view of Type-1

(c) Over view of Type-2

(d) Surface view of Type-2

(e) Spark's membership of Type-2

(f) Interval rule viewer of Type-2

Fig. 9. Graphical views of Type-1 and Type-2 fuzzy logic.

Table 6
Number of wins for different algorithms.

Problem	burma14	gr17	gr24	bayg29	dantzig42	swiss42	hk48	brazil58	eil76	gr96
T2FLDFWA	82	85	74	81	75	85	88	84	77	80
T1FLDFWA	78	73	64	75	62	70	74	81	69	69
GA	59	67	60	63	53	62	69	71	64	61

to the other. Therefore, Scheffe's multiple comparison F test is conducted to determine whether the results of T2FLDFWA and T1FLDFWA and/or T2FLDFWA and GA differ. For the pair, i.e., T2FLDFWA and GA, the calculated F value is obtained by $F = \frac{(\overline{X}_1 - \overline{X}_3)^2}{MS_W(\frac{1}{J}+\frac{1}{J})} = 67.78$. Similarly, for the other pair, i.e., T2FLDFWA and T1FLDFWA, the calculated F value is 16.34. As both calculated F values are greater than the tabulated value (3.35), there is a significant difference between T2FLDFWA and T1FLDFWA and between T2FLDFWA and GA. Therefore, it can be concluded that T2FLDFWA outperforms the other two algorithms. For the above reason, MrFPGRMs under different freshness functions and speeds Models 1–6 are solved by T2FLDFWA (coded in C-language and MATLAB R2015b) for some input data on a PC having IntelCorei5-4210U CPU with 1.70 GHz processor and 4.0 GB of RAM.

Table 7
Analysis of variance summary.
Source: Data taken from Table 6.

Source of variation	Sum of square	df	Mean of square	F
Between groups	$SS_B = 1657.8667$	$J-1=2$	$MS_B = \frac{SS_B}{J-1} = 828.9333$	
Within groups	$SS_W = 754.3021$	$J(I-1)=27$	$MS_W = \frac{SS_W}{J(I-1)} = 27.9371$	$\frac{MS_B}{MS_W} = 29.6714$
Total	$SS_T = 2412.1688$	29		

6. Numerical experiments: Solutions of Models (1–6) by T2FLDFWA

A routing problem with 10 nodes (1 depot and 9 retailers), 2 types of fruits, and 3 connecting routes among the nodes, and between the depot, and nodes (Fig. 1) is considered for illustration.

6.1. Input data

The values of the input parameters used in Models: 1–6 are given in Table 8 (cf. Micheli and Mantella (2018)).

Table 9 gives retailers' demands for two different products. In Table 10, distance matrix is given. Next, Table 11 furnishes the fixed carrying charges between the nodes for different routes. For Model-2, to calculate the average speed along each route, the minimum and maximum speed limits (a, d) for each route are given in Table 12.

6.2. Experimental outcomes

6.2.1. Optimum results of Models-1, 2, 3, 4, 5 and 6

With the abovementioned input data in Section 6.1, MrFPGRMs (Models: 1–6) defined in Section 3.3 are solved with the proposed T2FLDFWA. For the input data, the total unloading and purchasing costs are $ 56.00 and $ 1753.83, respectively. These values are the same for all models. In Tables 13 and 14, the results for the proposed models with different speeds and freshness functions are presented.

Model-1: The optimum routing plan is 1[3]-3[3]-4[3]-8[1]-7[3]-9[2]-6[3]-5[2]-10[2]-2[3]‖1,[5] which is pictorially represented by Fig. 10. The optimum average routing speed is 83.01 km/h with a profit of $ 610.61, and other parameters are evaluated and presented in Tables 13 and 14.

In doing so, during the journey from node 2 to node 1 via route 3 with an average speed of 83.01 km/h, the total duration of the trip is more than 2 h, and hence the driver takes a rest of 15 min just after a 2 h journey.

Model-2: For this model, the maximum profit and total travel time are $ 604.16 and 16.687 h, respectively. The optimum routing plan and optimum average speeds between the nodes are 1[1]-3[3]-4[3]-8[1]-7[3]-9[2]-6[3]-5[2]-10[2]‖2[3]‖1 and 83.10, 84.64, 74.55, 64.55, 67.78, 71.17, 72.92, 67.78, 52.78, 71.17 km/h, respectively. As maximum and minimum speed limits are imposed between every pair of nodes, optimum average speeds are restricted within those respective limits.

In this case, two driver's rests (‖) of 15 min are recorded, the first one in between nodes 10 and 2 via route 2 having a distance 160.00 km traveling with the speed 52.78 km/h and journey time is 3.03 h (more than 2 h). The second one is encountered between nodes 2 and 1 (depot) via route 3. Here, the journey time is more than 2 h because the travel distance and average speed are 200.00 km and 71.17 km/h, respectively.

Model-3: For this model, the optimum profit, average speed, and total travel time are $ 554.23, 70.84 km/h, and 16.291 h, respectively. The optimum routing plan is 1[3]-3[3]-4[3]-8[1]-7[3]-9[3]-6[3]-5[2]-10[2]‖2[3]‖1. Here, also two driver rests (‖) are also noted. The first one is between nodes 10 and 2 via route 2, with a distance of 160.00 km traveling with a speed of 70.84 km/h (the journey is for 2.26 h). The second one is between nodes 2 and 1 (depot) via route 3, with a journey time of more than 2 h for covering a distance of 200.00 km at a speed of 70.84 km/h.

Model-4: It is studied under varying speeds between two successive nodes with the formula for freshness as used in Model-2. The model furnishes the maximum profit of $ 562.70 along with a total travel time of 16.702 h. The optimum routing plan and speeds between nodes are 1[2]-8[0]-7[1]-9[2]-6[2]-3[2]-4[1]-2[2]‖10[1]-5[2]‖1 and 83.10, 84.64, 74.55, 69.55, 67.78, 71.17, 72.92, 67.78, 52.78, 71.17 km/h, respectively. Two driver rests (‖) are encountered between nodes 2 and 10 through route 2 and return from node 5 to the depot via route 2.

Model-5: In the proposed model, the fuel cost is minimized as an objective with Model-1's profit expression and specifications. From Tables 13 and 14, it is observed that the minimum fuel consumption is at the average routing speed of 43 km/h with a fuel cost of $ 223.09, which is lesser than the fuel cost $ 232.47 recorded at the same speed when profit is maximum for Model-1 in Table 16. Moreover, a fuel cost of $ 332.69 is incurred when a profit, $ 610.61, is achieved. Hence, it is clear from the optimum fuel cost analysis that the fuel cost is compromised for maximum profit. It is up to management to choose the best way to balance the trade-off between maximum profit and minimum fuel consumption. To better represent the nature of fuel cost against profit for different speed variations, Fig. 11 is given.

Four driver rests (‖) are noted during the minimum fuel cost tour. The first rest is encountered between the depot and node 8 via route 1, the second rest between nodes 4 and 2 through route 3, and the third and fourth rests while returning from node 2 to the depot via route 3.

Pareto front: In the multiobjective optimization, several compromised solutions (Pareto solutions) are obtained. It is impossible to obtain a single optimum solution from the above nondominated solution set. These solutions are obtained by varying the importance (weights) given to the objectives, and the Pareto front is depicted in Fig. 12(a). Here, the behavior of the objectives is different from other multiobjective optimization problems such as environmental cost and profit (De & Giri, 2020). Table 15 shows that profit reduces with fuel cost for increasing weights to fuel cost minimization. For more clarification, the graphical representation of profit and fuel cost wrt. weights (Fig. 12(b)) is presented. A compromised solution can be chosen depending upon the requirements of the decision-maker (wholesaler).

Model-6: Both fuel cost minimization and profit maximization are performed simultaneously as a multiobjective optimization problem. Utility function (Eq. (12)) is formulated with different weights. When $\varpi = 1$, this model reduces to Model-5, and on the other hand, when $\varpi = 0$, the model works like Model-1. Three more results are taken for $\varpi = 0.1$, $\varpi = 0.5$ and $\varpi = 0.9$. The results are summarized in Table 15.

6.2.2. Optimum results of Model 1 using the genetic algorithm

Model-1 is further solved by GA with probabilistic selection, cyclic crossover, and swap mutation operators for the same input data given in Section 6.1. The average travel speed throughout the routes is 81.00

[5] The routing plan 1[3]-3[3]-4[3]-8[1]-7[3]-9[2]-6[3]-5[2]-10[2]-2[3]‖1 (the number inside the third brackets indicates the route number, the number outside of the brackets represents the node and ‖ indicates driver's rest), means that the driver starts from node 1 (depot) and goes to the node 3 traveling through route 3. After that, node 4 is visited via route 3, and in this way, at last, node 1 (depot) is visited from node 2 via route 3.

Table 8
Input parameters for the proposed models.

Notation	Values	Notation	Values	Notation	Values	Notation	Values
Ω^1	0.002	S^2	0.8929	L	1.3730	ψ	737
Ω^2	0.0022	P^1	0.5083	tim^1	40	g	9.81
t^1	0.00139	P^2	0.3846	tim^2	50	κ	44
t^2	0.00111	D_s	2.7476	t''	0.25	ϕ	0
α^1	0.01373	F_a	7.0	c_d	0.6	ω	0.45
α^2	0.01511	V_c	4000	c_r	0.01	τ	0
ϑ_1	30	N_e	38.3	μ	3500	ρ	1.2041
ϑ_2	90	K_e	0.258	ϵ	0.45		
S^1	0.9616	V_e	4.50	ξ	1		

Table 9
Demand matrix (kg).

Retailers	1	2	3	4	5	6	7	8	9	10
Product 1	0	250	300	150	245	275	160	280	190	220
Product 2	0	100	170	299	200	150	280	160	190	275

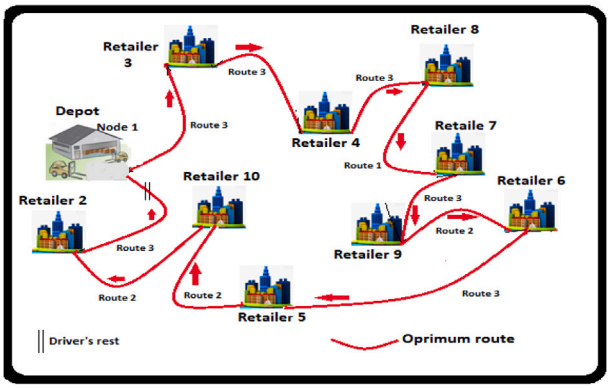

Fig. 10. Optimum route for Model-1.

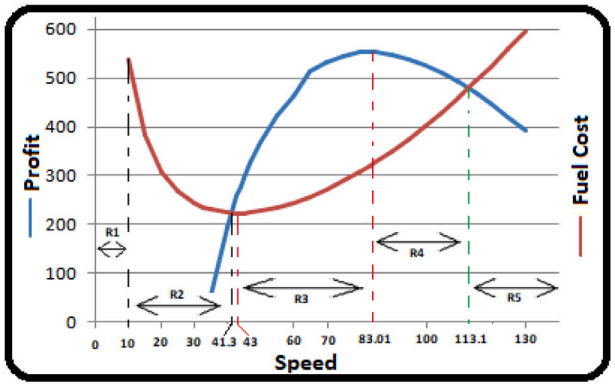

Fig. 11. Fuel Cost vs. Profit for Model-5.

km/h with a profit of $ 610.48, and other results are presented in Tables 13 and 14. It is seen from the above two tables that the profit for Model-1 is slightly better in the case of T2FLDFWA than the GA. The optimal routing plan and average velocities are also different in the GA.

7. Parametric analysis

Some parameters — goods carrying cost of $ 342.60, a total distance of 758.40 km, fixed carrying cost of $ 161.01, and fixed charge of $ 1.92 remain unchanged throughout this analysis, which is performed on Model-1.

7.1. Nature of costs, revenue, and profit (Fig. 13)

The proposed Model-1 is further dissected against different values of the vehicle's average speed, and the results are summarized in Table 16. Fig. 13 is the pictorial representation of Table 16, showing the changes in revenue, total cost, fuel cost, driver salary, and profit against different speeds of the vehicle.

- Costs: Out of the costs, purchasing and unloading costs are fixed, i.e., independent of travel time/speed for the model. Here, fuel cost and driver salary and hence the total cost change with speed. From Fig. 13, the driver's salary gradually decreases with speed. As the driver is on per hour salary, the driver gets less salary for fewer working hours. Thus, the driver salary decreases with speed because higher speed reduces the total travel time.

  Here, toward the beginning (with low speed), the fuel cost decreases with an increase in speed, reaches a minimum, and then increases. This pattern is as per the nature of the fuel consumption of a running vehicle. As fuel the cost dominates over all other variable costs, the behavior of the total cost is the same as that of the fuel cost.

- Revenue: Revenue, i.e., the selling price of the items, increases with speed. Initially, this increase is very sharp and then slow. This is because an item's freshness is time dependent, initially decreasing slowly and then very quickly.

- Profit: The nature of the profit (revenue ≥ 0) is the same as revenue but moderated by speed-dependent costs. After a certain speed, revenue increases very slowly and profit decreases.

- Costs, Revenue, and Profit within specific speed intervals:

  Here, the vehicle's velocity range is divided into some intervals, R1–R6, and within each interval, the nature of the model's components — profit, costs, etc., are discussed.

  In R1 (0–10 km/h), it is not feasible to run the vehicle at such a low speed.

  In R2 (10–32.41 km/h), within this interval, with a decrease in travel time, fuel cost and driver's salary decrease sharply (thus, total cost decreases). On the other hand, the increase in revenue is also very fast. Due to slow speed, the total cost (including fixed costs) is high, and the corresponding profit is negative. Here, the revenue increase rate is much higher than the decrease in total cost. At a speed of 32.41 km/h, revenue and total cost are equal; hence, profit is zero.

  In R3 (32.41–44 km/h), at 32.41 km/h, the trade-off between revenue and total cost commences. After this point, revenue increases, and total cost decreases. The total cost is minimum at speed 44 km/h. In-between (33.0–34.0) km/h speed, profit, and driver's salary are equal. In this region, fuel cost is minimum at 43.0 km/h, which is different from the total cost minimum point (44.0 km/h) because of the driver's salary. After 43.0 km/h, both profit and fuel cost increase.

Table 10
Distance matrix along different routes (km).

i/j	1	2	3	4	5
1	∞	(240.0, 216.0, 200.0)	(132.4, 136.0, 132.4)	(132.8, 131.6, 135.6)	(134.4, 130.0, 138.4)
2	(240.0, 216.0, 200.0)	∞	(158.0, 152.0, 160.4)	(162.4, 159.6, 152.0)	(404.0, 428.0, 460.0)
3	(132.4, 136.0, 132.4)	(158.0, 152.0, 160.4)	∞	(16.0, 28.0, 12.0)	(190.4, 172.8, 192.8)
4	(132.8, 131.6, 135.6)	(162.4, 159.6, 152.0)	(16.0, 28.0, 12.0)	∞	(139.2, 132.6, 130.2)
5	(134.4, 130.0, 138.4)	(404.0, 428.0, 460.0)	(190.4, 172.8, 192.8)	(139.2, 132.6, 130.2)	∞
6	(146.0, 148.4, 143.6)	(293.0, 306.0, 289.0)	(46.6, 47.8, 49.0)	(164.5, 168.7, 159.6)	(53.2, 50.2, 54.2)
7	(148.8, 148.0, 147.2)	(150.8, 155.6, 144.0)	(60.6, 58.2, 59.8)	(152.0, 147.5, 155.5)	(54.8, 50.8, 44.8)
8	(126.4, 124.2, 122.8)	(172.4, 168.0, 169.2)	(65.4, 66.2, 62.8)	(65.6, 62.0, 58.6)	(64.8, 69.6, 62.4)
9	(148.6, 212.4, 220.0)	(147.4, 148.2, 144.0)	(162.8, 167.2, 168.4)	(163.2, 156.0, 164.8)	(43.6, 41.2, 40.0)
10	(220.4, 215.2, 217.2)	(157.2, 160.0, 154.2)	(216.8, 220.4, 212.0)	(217.2, 210.4, 220.4)	(54.6, 56.4, 60.2)
i/j	6	7	8	9	10
1	(146.0, 148.4, 143.6)	(148.8, 148.0, 147.2)	(126.4, 124.2, 122.8)	(148.6, 212.4, 220.0)	(220.4, 215.2, 217.2)
2	(293.0, 306.0, 289.0)	(150.8, 155.6, 144.0)	(172.4, 168.0, 169.2)	(147.4, 148.2, 144.0)	(157.2, 160.0, 154.2)
3	(46.6, 47.8, 49.0)	(60.6, 58.2, 59.8)	(65.4, 66.2, 62.8)	(162.8, 167.2, 168.4)	(216.8, 220.4, 212.0)
4	(164.5, 168.7, 159.6)	(152.0, 147.5, 155.5)	(65.6, 62.0, 58.6)	(163.2, 156.0, 164.8)	(217.2, 210.4, 220.4)
5	(53.2, 50.2, 54.2)	(54.8, 50.8, 44.8)	(64.8, 69.6, 62.4)	(43.6, 41.2, 40.0)	(54.6, 56.4, 60.2)
6	∞	(36.4, 40.8, 34.4)	(64.4, 68.8, 63.6)	(36.4, 34.0, 39.2)	(46.4, 44.8, 42.2)
7	(36.4, 40.8, 34.4)	∞	(27.2, 30.4, 32.8)	(31.6, 26.0, 23.6)	(56.8, 64.4, 60.4)
8	(64.4, 68.8, 63.6)	(27.2, 30.4, 32.8)	∞	(44.8, 38.0, 42.0)	(49.2, 55.2, 46.4)
9	(36.4, 34.0, 39.2)	(31.6, 26.0, 23.6)	(44.8, 38.0, 42.0)	∞	(67.2, 60.4, 72.8)
10	(46.4, 44.8, 42.2)	(56.8, 64.4, 60.4)	(49.2, 55.2, 46.4)	(67.2, 60.4, 72.8)	∞

Table 11
Fixed carrying cost(C^0_{ijr}) matrix ($)

i/j	1	2	3	4	5
1	∞	(9.0671, 8.2428, 7.8994)	(20.6759, 17.9969, 15.5241)	(21.2254, 18.8899, 20.6759)	(21.7749, 22.3244, 21.9810)
2	(9.0671, 8.2428, 7.8994)	∞	(22.0497, 21.6375, 22.6679)	(23.4235, 22.6679, 24.0417)	(11.6087, 10.5783, 11.8835)
3	(20.6759, 17.9969, 15.5241)	(22.0497, 21.6375, 22.6679)	∞	(7.5559, 6.1821, 9.6167)	(34.7575, 33.6584, 35.8565)
4	(21.2254, 18.8899, 20.6759)	(23.4235, 22.6679, 24.0417)	(7.5559, 6.1821, 9.6167)	∞	(28.2318, 27.5449, 28.9188)
5	(21.7749, 22.3244, 21.9810)	(11.6087, 10.5783, 11.8835)	(34.7575, 33.6584, 35.8565)	(28.2318, 27.5449, 28.9188)	∞
6	(26.0337, 24.0417, 26.4459)	(29.3309, 30.5673, 28.8501)	(35.4444, 34.0706, 34.9635)	(29.2622, 21.7749, 21.0880)	(33.3150, 32.4220, 26.9267)
7	(27.2015, 26.5146, 26.8580)	(18.6151, 19.1647, 19.4394)	(18.2717, 24.0417, 23.3548)	(18.4091, 17.2413, 23.9043)	(20.8132, 21.6375, 22.0497)
8	(28.1632, 34.2766, 28.9874)	(27.3389, 28.7127, 26.1024)	(21.2941, 15.1119, 27.4763)	(22.0497, 15.8675, 21.8436)	(24.4539, 25.0721, 23.1487)
9	(31.1856, 30.6360, 36.4060)	(22.5992, 14.7685, 20.8819)	(27.4076, 18.5465, 33.2463)	(27.3389, 33.0402, 35.0322)	(32.9028, 32.2846, 33.5210)
10	(36.4747, 32.9715, 31.0482)	(29.4683, 21.5688, 29.9491)	(33.5210, 32.3533, 31.5977)	(33.9332, 33.1776, 34.2766)	(27.4763, 21.6375, 28.0945)
i/j	6	7	8	9	10
1	(26.0337, 24.0417, 26.4459)	(27.2015, 26.5146, 26.8580)	(28.1632, 34.2766, 28.9874)	(31.1856, 30.6360, 36.4060)	(36.4747, 32.9715, 31.0482)
2	(29.3309, 30.5673, 28.8501)	(18.6151, 19.1647, 19.4394)	(27.3389, 28.7127, 26.1024)	(22.5992, 14.7685, 20.8819)	(29.4683, 21.5688, 29.9491)
3	(35.4444, 34.0706, 34.9635)	(18.2717, 24.0417, 23.3548)	(21.2941, 15.1119, 27.4763)	(27.4076, 18.5465, 33.2463)	(33.5210, 32.3533, 31.5977)
4	(29.2622, 21.7749, 21.0880)	(18.4091, 17.2413, 23.9043)	(22.0497, 15.8675, 21.8436)	(27.3389, 33.0402, 35.0322)	(33.9332, 33.1776, 34.2766)
5	(33.3150, 32.4220, 26.9267)	(20.8132, 21.6375, 22.0497)	(24.4539, 25.0721, 23.1487)	(32.9028, 32.2846, 33.5210)	(27.4763, 21.6375, 28.0945)
6	∞	(13.7381, 12.9825, 14.9058)	(24.3165, 23.6983, 23.0800)	(12.3643, 14.4250, 13.5320)	(35.0322, 34.2766, 35.6505)
7	(13.7381, 12.9825, 14.9058)	∞	(10.2349, 10.6470, 9.6167)	(11.8835, 12.5017, 11.3339)	(22.0497, 21.2254, 21.9123)
8	(24.3165, 23.6983, 23.0800)	(10.2349, 10.6470, 9.6167)	∞	(16.8979, 17.2413, 16.8292)	(18.6151, 18.2030, 17.2413)
9	(12.3643, 14.4250, 13.5320)	(11.8835, 12.5017, 11.3339)	(16.8979, 17.2413, 16.8292)	∞	(25.3468, 25.5529, 24.3852)
10	(35.0322, 34.2766, 35.6505)	(22.0497, 21.2254, 21.9123)	(18.6151, 18.2030, 17.2413)	(25.3468, 25.5529, 24.3852)	∞

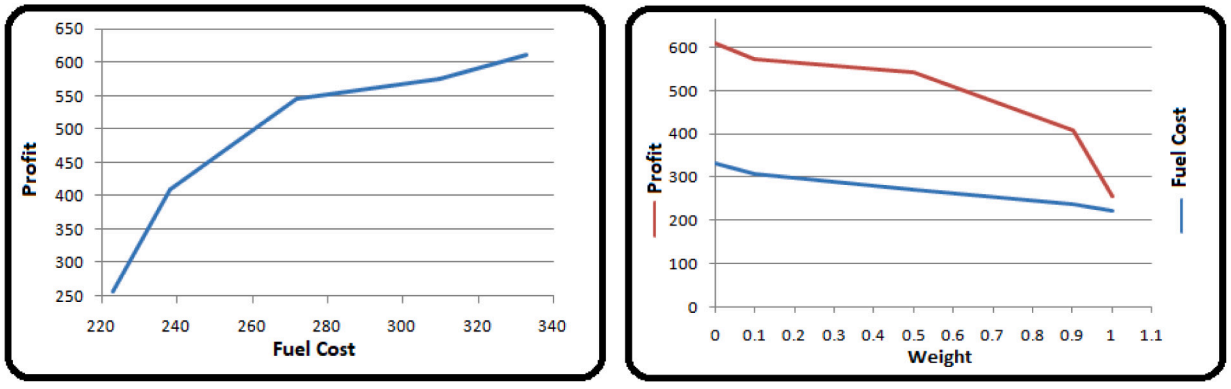

(a) Pareto front (b) Profit and Fuel cost against different weights

Fig. 12. Results of Model-6.

In R4 (44–83.01 km/h), profit is maximum at 83.01 km/h; after this, a trade-off between profit and fuel cost commences. In this range, the gap between revenue and total cost widens. After 83.01 km/h this gap slowly decreases.

Table 12
Maximum and minimum speed matrix for different routes (km/h).

i/j	1	2	3	4	5
1	((0, 0),(0, 0),(0, 0))	((25, 70),(30, 75),(40, 95))	((20, 120),(35, 80),(20, 50))	((40, 80),(25, 95),(35, 55))	((40, 75),(30, 90),(20, 70))
2	((20, 60),(50, 100),(45, 70))	((0, 0),(0, 0),(0, 0))	((30, 100),(45, 70),(60, 120))	((40, 100),(35, 90),(45, 95))	((50, 85),(25, 95),(45, 95))
3	((35, 100),(40, 75),(35, 85))	((30, 55),(45, 65),(60, 100))	((0, 0),(0, 0),(0, 0))	((35, 55),(45, 95),(65, 90))	((45, 120),(25, 45),(55, 85))
4	((45, 95),(40, 85),(25, 55))	((30, 50),(65, 80),(45, 90))	((35, 85),(45, 70),(55, 80))	((0, 0),(0, 0),(0, 0))	((30, 50),(45, 90),(30, 80))
5	((50, 100),(50, 95),(65, 85))	((40, 75),(35, 85),(50, 80))	((40, 80),(60, 120),(25, 55))	((45, 85),(25, 70),(35, 85))	((0, 0),(0, 0),(0, 0))
6	((45, 85),(35, 90),(40, 75))	((50, 120),(45, 100),(35, 75))	((45, 95),(55, 85),(30, 70))	((45, 85),(50, 100),(35, 65))	((40, 110),(45, 80),(40, 95))
7	((35, 80),(40, 90),(50, 100))	((45, 90),(35, 85),(45, 75))	((40, 120),(35, 70),(50, 100))	((45, 85),(30, 70),(45, 90))	((35, 80),(50, 120),(45, 75))
8	((35, 80),(45, 85),(40, 95))	((40, 85),(50, 100),(30, 90))	((40, 85),(25, 60),(45, 80))	((35, 95),(50, 90),(45, 110))	((40, 85),(30, 70),(40, 85))
9	((30, 70),(45, 100),(50, 95))	((30, 70),(45, 100),(40, 95))	((55, 110),(35, 90),(50, 85))	((45, 110),(40, 85),(35, 85))	((55, 120),(40, 85),(30, 65))
10	((35, 75),(40, 110),(50, 95))	((45, 85),(30, 70),(55, 120))	((45, 95),(35, 90),(40, 95))	((50, 100),(40, 95),(35, 85))	((45, 95),(50, 85),(35, 75))
i/j	6	7	8	9	10
1	((15, 40),(45, 85),(30, 80))	((45, 115),(35, 85),(30, 90))	((25, 55),(40, 85),(30, 100))	((50, 95),(30, 120),(45, 80))	((20, 75),(50, 70),(45, 90))
2	((25, 65),(30, 55),(40, 65))	((25, 45),(45, 95),(50, 90))	((45, 90),(30, 65),(50, 75))	((25, 40),(45, 85),(40, 95))	((30, 50),(55, 95),(40, 70))
3	((45, 65),(40, 85),(35, 95))	((55, 80),(60, 85),(35, 95))	((40, 95),(55, 105),(40, 90))	((50, 80),(65, 100),(25, 40))	((55, 80),(40, 85),(35, 95))
4	((55, 95),(25, 70),(55, 100))	((50, 75),(40, 110),(45, 90))	((45, 85),(40, 85),(45, 95))	((50, 120),(60, 80),(45, 90))	((50, 90),(35, 65),(35, 85)))
5	((45, 65),(25, 65),(55, 95))	((45, 95),(55, 110),(65, 90))	((45, 65),(35, 65),(30, 90))	((40, 70),(45, 95),(35, 75))	((50, 90),(45, 85),(40, 80))
6	((0, 0),(0, 0),(0, 0))	((45, 90),(35, 75),(50, 110))	((45, 80),(30, 85),(40, 90))	((30, 90),(50, 100),(25, 65))	((40, 80),(30, 80),(50, 120))
7	((35, 80),(50, 110),(40, 95))	((0, 0),(0, 0),(0, 0))	((40, 90),(45, 85),(50, 120))	((35, 75),(50, 95),(45, 85))	((45, 110),(30, 80),(45, 95))
8	((45, 90),(50, 90),(40, 85))	((35, 75),(40, 90),(50, 95))	((0, 0),(0, 0),(0, 0))	((35, 80),(45, 85),(50, 120))	((40, 90),(35, 85),(45, 85))
9	((35, 75),(45, 90),(35, 85))	((40, 110),(50, 120),(45, 75))	((30, 80),(35, 85),(50, 85))	((0, 0),(0, 0),(0, 0))	((40, 75),(50, 110),(55, 110))
10	((45, 85),(40, 110),(45, 95))	((40, 110),(50, 100),(35, 65))	((30, 85),(35, 75),(50, 95))	((45, 90),(50, 85),(35, 75))	((0, 0),(0, 0),(0, 0))

Table 13
Optimum results of the Models-1, 2, 3, 4 and 5.

Method	Model	Total distance covered	Total travel time	Goods carrying cost	Fixed carrying cost	Fuel cost	Fixed charge	Driver rest	Driver salary	Selling price	Total transportation cost	Profit
T2FLDFWA	1	758.40	14.398	342.60	161.01	332.69	1.92	1	39.56	3298.22	2687.61	610.61
–	2	758.40	16.687	342.60	166.16	284.92	2.19	2	45.85	3255.71	2651.55	604.16
–	3	763.59	16.291	345.37	160.11	287.01	1.92	2	44.76	3203.23	2649.0	554.23
–	4	761.59	16.702	345.37	166.57	286.65	2.19	2	45.89	3219.20	2656.50	562.70
–	5	728.20	22.919	354.54	223.17	223.09	2.06	4	62.97	2933.36	2675.63	257.73
GA	1	754.40	14.576	341.21	166.50	322.25	1.92	1	40.05	3292.24	2681.79	610.48

Table 14
Optimum routing plan and speed of the Models-1, 2, 3, 4 and 5.

Method	Model	Average speed along different routes	Optimum routing plan
T2FLDFWA	1	← 83.01 →	1[3]-3[3]-4[3]-8[1]-7[3]-9[2]-6[3]-5[2]-10[2]-2[3]‖1
–	2	83.10, 84.64, 74.55, 64.55, 67.78, 71.17, 72.92, 67.78, 52.78, 71.17	1[1]-3[3]-4[3]-8[1]-7[3]-9[2]-6[3]-5[2]-10[2]‖2[3]‖1
–	3	← 70.84 →	1[3]-3[3]-4[3]-8[1]-7[3]-9[3]-6[3]-5[2]-10[2]‖2[3]‖1
–	4	83.10, 84.64, 74.55, 69.55, 67.78, 71.17, 72.92, 67.78, 52.78, 71.17	1[2]-8[0]-7[1]-9[2]-6[2]-3[2]-4[1]-2[2]‖10[1]-5[2]‖1
–	5	← 43.00 →	1[1]‖8[1]-7[2]-9[3]-5[1]-10[3]-6[2]-3[3]-4[3]‖2[3]‖‖1
GA	1	← 81.00 →	1[3]-3[3]-4[3]-8[1]-7[3]-9[2]-6[2]-5[2]-10[2]-2[3]‖1

Table 15
Optimum results for multiobjective Model-6.

Weight	Fuel cost	Profit
0.0	332.69	610.61
0.1	309.74	574.85
0.5	271.70	544.68
0.9	238.05	410.25
1.0	223.09	257.73

In R5 (83.01–115.9 km/h), revenue, total cost, and fuel cost increase, but both profit and driver's salary decrease. At 115.9 km/h, profit and fuel cost are equal.

In R6 (115.9–130 km/h), the nature of all costs, revenue, and profit are the same as in R5.

7.2. Trade-off between profit and fuel cost wrt. Figs. 13 and 11

A transportation system's fuel cost and profit are usually expected to be conflicting, i.e., if fuel cost increases, profit decreases, and vice versa. For the present model, the confrontation of fuel cost and profit can be classified into three groups wrt. velocity intervals (i) if average velocity is in 10–43.0 km/h, profit increases and fuel cost decreases (fuel cost is minimum at 43.0 km/h speed), (ii) for 43.0–83.01 km/h, both fuel cost and profit increase (profit is maximum at 83.01 km/h) and (iii) after 83.01 km/h speed, profit decreases, and fuel cost increases. All these different profit and fuel cost behaviors are due to the change in freshness over time and the vehicle's fuel consumption technology. An interesting profit and fuel cost behavior pattern is noted in the range 43.00 to 83.01 km/h, where both fuel cost and profit increase. In general, increased fuel cost reduces profit. However, in this case, profit increases with fuel cost. This is because the selling price (revenue) overpowers the total cost (fuel cost). There exists a trade-off between profit and fuel cost within this speed region. Later, this is further explained through multiobjective formulation, i.e., simultaneous maximization of profit and minimization of fuel cost. Moreover, from the graph of revenue (which represents profit) and total cost (which includes fuel cost) in Fig. 13, the gap between these two widens within this speed region. This implies that the revenue increase rate is much higher than that of the total cost, which is also evident from Table 16. The nature of the trade-off of profit and fuel cost wrt. Fig. 11 (against minimization of fuel cost) is the same as in Fig. 13, only the difference is in the maximum and minimum values of profit ($ 553.24) and fuel cost ($ 223.09) respectively. All these are observed against the same average vehicle speed as in Fig. 13 (profit maximization).

7.3. Minimum carbon emission vs. Minimum total cost

Although fuel cost is the vital component of the total cost, the minimum fuel cost is at 43.0 km/h speed, but the total cost is minimum at 44.0 km/h speed (Fig. 13). This is due to the driver's salary (another component of total cost), which decreases with time. If the wholesaler is more sensitive to carbon emissions, the journey should be completed at 43.0 km/h. On the other hand, if the wholesaler is very serious about the total cost, then a 44.0 km/h speed is suitable. Of course, these two speeds do not fetch the maximum profit. For the reason mentioned above, routing (journey) should be completed with an average speed of 83.01 km/h.

7.4. Effects of unloading time on profit and selling price

For analysis of the impact of the unloading time of items on profit and freshness (selling price), Table 17 is presented. It is shown in the above table that profit ranges from $ 739.03 to $ 461.57, and the corresponding selling price changes from $ 3419.90 to $ 3155.91 as unloading time varies from 50% to 150%. For a better illustration of the relation between unloading time, profit, and selling price, Fig. 14 is added. Hence, it can be concluded that both the time-dependent selling price of items and the profit are more sensitive to a change in unloading time.

7.5. Importance of route for the system

Here, for the first time, different route connections between cities are considered in the fresh produce distribution system. Table 18 illustrates the importance of multiple routes between two nodes (cities) for maximum profit. For Model-1, the optimum routing plan 1[3]-3[3]-4[3]-8[1]-7[3]-9[2]-**6[3]-5**[2]-10[2]-2[3]‖1 is chosen with total covered distance of 758.40 km (Tables 13 and 14). When slightly shorter distanced routing plans are considered, the corresponding profits do not improve.

For instance, for 1[3]-3[3]-4[3]-8[1]-7[3]-9[2]-**6[1]-5**[2]-10[2]-2[3]‖1 with a total distance of 757.40 km, the recorded profit is $ 605.52, which is less than the optimum profit of $ 610.61 (Tables 13 and 14). Here, the distance from node 6 to node 5 via route 1 (53.2 km) is shorter than the distance from node 6 to node 5 via route 3 (54.2 km). Due to this change in route, the selling price is increased, and the goods carrying cost, driver salary, and fuel cost are decreased, but there is a significant increase in the fixed carrying cost. This increase dominates the other decreases, and due to that, total profit is less than the optimum profit. Thus, smaller distanced routes do not always fetch more profit. Despite the availability of shorter routes, the proposed model takes a route with a larger distance for maximum profit.

Four more available routing plans with smaller distances are considered to support the argument (shorter distances do not always fetch the maximum profit), and the results are presented along with the corresponding parameters in Table 18.

7.6. Profit against fuel cost

From the results in Table 16, profit is graphically represented against fuel cost and pictorially illustrated in Fig. 15. It is interesting to note that profit sharply increases for a small interval of fuel cost ($ 232.47 to $ 282.22). However, once it attains the maximum value, profit decreases slowly with the increase in fuel cost. This behavior is due to the vehicle's speed and design concept for optimum fuel consumption.

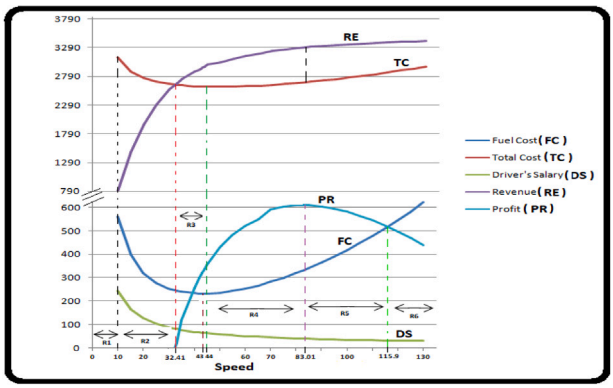

Fig. 13. Results for Model-1.

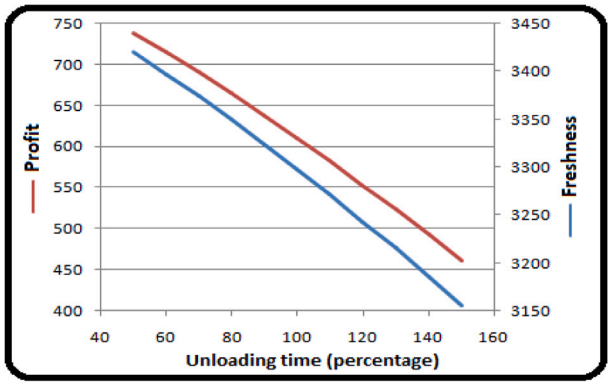

Fig. 14. Profit analysis against unloading time.

Table 16
Profit and Fuel cost wrt. speed analysis.

Speed	Total travel time	Fuel cost	Driver rest	Driver salary	Selling price	Total transportation cost	Profit
33	29.744	244.07	7	81.72	2662.91	2641.15	21.76
42	24.069	232.60	4	66.13	2914.00	2614.09	299.91
43	23.649	232.47	4	64.98	2932.33	2612.78	319.55
44	23.249	232.53	4	63.88	2949.73	2611.77	337.96
70	16.347	282.22	2	44.91	3234.10	2642.49	591.61
83	14.400	332.65	1	39.57	3298.18	2687.58	610.60
83.01	14.398	332.69	1	39.56	3298.22	2687.61	610.61
84	14.291	337.10	1	39.26	3301.96	2691.72	610.24
100	12.596	418.74	0	34.61	3350.47	2768.71	581.76
130	10.846	620.84	0	29.80	3404.88	2966.00	438.88

Table 17
Unloading time based analysis.

Unloading time	Total travel time	Driver salary	Selling price	Total transportation cost	Profit
50%	11.948	32.82	3419.90	2680.87	739.03
70%	12.928	35.52	3374.05	2683.57	690.48
90%	13.900	38.21	3324.38	2686.26	638.12
100%	14.398	39.56	3298.22	2687.61	610.61
110%	14.889	40.90	3271.24	2688.95	582.29
130%	15.869	43.60	3214.96	2691.65	523.31
150%	16.849	46.29	3155.91	2694.34	461.57

7.7. Profit sharing against continuous driving risk

For a risk-free journey, the driver should take 15 min to rest every 2 h of continuous driving (Tucker et al., 2003; Wang & Pei, 2014). Continuous driving without rest invites risks (accident) for both the

Table 18
Parametric analysis of Model-1 wrt. different routes.

Total distance covered	Total travel time	Goods carrying cost	Fixed carrying cost	Fuel cost	Driver salary	Selling price	Total transportation cost	Profit	Optimum routing plan
758.40	**14.398**	**342.60**	**161.01**	**332.69**	**39.56**	**3298.22**	**2687.61**	**610.61**	**1 [3] -3 [3] -4 [3] -8 [1] -7 [3] -9 [2] -6 [3] -5 [2] -10 [2] -2 [3] ‖1**
757.40	14.386	342.26	167.39	332.25	39.52	3298.69	2693.17	605.52	1[3]-3[3]-4[3]-8[1]-7[3]-9[2]-6[1]-5[2]-10[2]-2[3]‖1
754.40	14.35	341.21	166.50	330.92	39.43	3300.10	2689.81	610.29	1[3]-3[3]-4[3]-8[1]-7[3]-9[2]-6[2]-5[2]-10[2]-2[3]‖1
756.59	14.377	342.52	166.84	331.89	39.50	3298.81	2692.50	606.31	1[3]-3[3]-4[3]-8[1]-7[3]-9[2]-6[3]-5[1]-10[2]-2[3]‖1
755.59	14.365	342.60	168.91	331.46	39.47	3298.63	2694.19	604.44	1[3]-3[3]-4[3]-8[1]-7[3]-9[2]-6[3]-5[2]-10[1]-2[3]‖1
752.59	14.329	342.60	169.39	330.14	39.37	3299.06	2693.25	605.81	1[3]-3[3]-4[3]-8[1]-7[3]-9[2]-6[3]-5[2]-10[3]-2[3]‖1

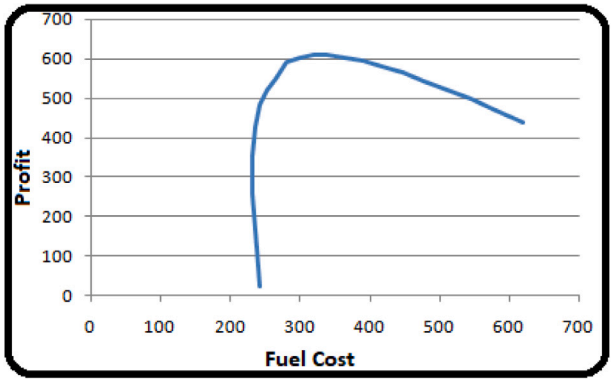

Fig. 15. Fuel Cost vs. Profit.

driver (life risk) and wholesaler (vehicle damage, compensation against death, etc.). This extra time (driver's rest) plays an important role in profit maximization in the fresh produce distribution system. If the driver's rest is allowed, the journey is safe, but the freshness of the items goes down at subsequent nodes, and hence profit is reduced. Against some risk of both parties (wholesaler and driver) for nonstop journey after 2 h, the profit will be more, and the wholesaler may share a part of that profit with the driver.

Here, three different scenarios are presented: (i) with driver's rest at due time, (ii) without the concept of diver's rest, and (iii) with driver's rest taken not at the due places (journey time is exactly two hours) but at the subsequent node. In the case of the third scenario, the driver takes some risks without taking rest when it is needed. Here, profit is more due to the increased freshness of items, and a part of this excess profit can be shared with the driver as an incentive.

Scenario-(i): Results of Models: 1–5 (presented thus far in the Tables 13 and 14) and Model-6 are with driver rest at due time. The results of Models: 1–4 are also given in Table 19.

Scenario-(ii): In this scenario, there is no concept of driver rest, i.e., it is assumed that even if a driver drives a vehicle continuously for a long time without any rest, they do not face any risk. For the present routing model, it is assumed that the driver drives without rest from one node to another without any risk, and the outcomes are listed in Table 19.

Scenario-(iii): In this scenario, the driver does not break their journey between two nodes and, in some cases, drives with risks even after 2 h. Instead of resting when they are supposed to, the driver takes rests for 15 min at the subsequent node during unloading of the products. Here, risks are measured by the excess time over a 2 h journey.

For Model-1, only one driver rest is encountered between nodes 2 and 1 (depot) via route 3 (returning from the last node to the depot). Therefore, in this case, only two scenarios ((i) and (ii)) are observed. Table 19 presents the scenarios with driver's rest and without driver rest. As the driver's rest is on the way to return to the depot, it does not affect the item's freshness (revenue). Only the driver's salary of 15 min driving is saved by the wholesaler. Hence, the wholesaler's profit is increased by an amount of $ 0.69 under Scenario-(ii).

Model-2 has two driver rests; the first is between nodes 10 and 2 through route 2 and the second is during the return to depot from node 2 via route 3. Profit-sharing scenarios- (i), (ii) and (iii) are presented in Table 19. With no driver's rest, an additional profit of $ 4.53 can be earned by the wholesaler. Whereas, with the driver's rest under Scenario-(iii), an excess profit of $ 3.15 is made with some risk. Here, profit share lies in between $ 0 and $ 3.15.

In Model-3, like Model-2, two driver's rests are observed between nodes 10 and 2 via route 2 and during the return journey, from node 2 to the depot through route 3. Outcomes under three scenarios (i), (ii) and (iii) are given in Table 19. As before, with no driver's rest, an additional profit of $ 3.05 is earned by the wholesaler. However, with driver's rest under Scenario (iii), an excess profit of $ 1.67 is made with some risk. Here, the profit share lies between $ 0 and $ 1.67.

Model-4 also has two driver's rests, and the results under scenarios (i), (ii), and (iii) are presented in Table 19. Without the driver's rest, the wholesaler makes an additional profit of $ 3.08. However, if the driver takes rest at the next node 10 rather than in between nodes 2 and 10 via route 2, an excess of $ 1.70 can be earned with some risk. The driver can agree to follow Scenario-(iii) to share the profit of $ 0 and $ 1.70.

7.8. Level of risk against continuous driving

A new model, Model-2a, is considered and analyzed under Scenario-(iii). It is the same as Model-2 with a different distance matrix (Table 20). Other input parameters remain unchanged. The optimum routing plan and speeds at the corresponding routes are 1[1]‖3[2]-6[2]-9[3]-7[1]-8[3]-10[2]-5[1]‖4[3]‖2[3]‖1 and 83.10, 66.17, 79.55, 67.78, 69.55, 67.78, 69.38, 67.78, 71.17, 71.17 km/h, respectively. The optimum profit is $ 272.00, the total distance covered is 929.00 km, the total travel time is 18.905 h, the goods carrying cost is $ 430.25, the fixed carrying cost is $ 189.79, the fuel cost is $ 357.97, fixed charge is $ 2.19, the driver salary is $ 51.94, the selling price is $ 3113.97, the total transportation cost is $ 2841.97 and 4 driver rests are encountered. These are between nodes 1 and 3 via route 1, nodes 5 and 4 via route 1, nodes 4 and 2 via route 3, and during the return journey, from node 2 to the depot (node 1) through route 3. For ease of representation, the first three rests are denoted by $\varphi 1$, $\varphi 2$, and $\varphi 3$, respectively. Table 21 presents results related to profit and risks. For cases 4, 5, 6, and 7, excess running times for not taking rests at different due rest positions are added. For instance, under case-4, these two forced rest positions are at nodes 3 and 2, and the total cumulative risk is calculated, adding the risk times under cases 1 and 2. Similar is the case for cases 5, 6 and 7. Here, the level of risk is classified on a scale and mentioned against each case.

8. Practical implementation and managerial insights

Here, a real-life wholesaler's fruit distribution in West Bengal, India, is presented. Around Kolkata, West Bengal, papaya[6] and Litchi (Mitra & Pathak, 2008) are grown in 24-Parganas and M/s. Gazi fruit

[6] http://surl.li/dlplx.

Table 19
Parametric analysis of Models-1, 2, 3 and 4 for profit sharing schemes.

Model	Scenario	Total distance covered	Total travel time	Goods carrying cost	Fixed carrying cost	Fuel cost	Fixed charge	Driver rest	Driver salary	Selling price	Total transportation cost	Profit	Amount of risk (h)
1	i	758.40	14.398	342.60	161.01	332.69	1.92	1	39.56	3298.22	2687.61	610.61	0
	ii							0	38.87	3298.22	2686.92	611.30	–
2	i	758.40	16.687	342.60	166.16	284.92	2.19	2	45.85	3255.71	2651.56	604.16	0
	ii							0	44.47	3258.86	2650.17	608.69	–
	iii							2	45.85	3258.86	2651.55	607.31	1.031
3	i	763.59	16.291	345.37	160.11	287.01	1.92	2	44.76	3203.23	2649.0	554.23	0
	ii							0	43.38	3204.90	2647.62	557.28	–
	iii							2	44.76	3204.90	2649.00	555.90	0.258
4	i	761.59	16.702	345.37	166.57	286.65	2.19	2	45.89	3219.21	2656.50	562.70	0
	ii							0	44.51	3220.90	2655.12	565.78	–
	iii							2	45.89	3220.90	2656.50	564.40	0.360

Table 20
Adjusted distance matrix for Model- 2a (km).

i/j	1	2	3	4	5
1	∞	(240.0, 216.0, 200.0)	(172.4, 176.0, 172.4)	(182.8, 181.6, 185.6)	(174.4, 170.0, 178.4)
2	(240.0, 216.0, 200.0)	∞	(158.0, 152.0, 160.4)	(162.4, 159.6, 152.0)	(404.0, 428.0, 460.0)
3	(172.4, 176.0, 172.4)	(158.0, 152.0, 160.4)	∞	(160.0, 158.0, 172.0)	(190.4, 172.8, 192.8)
4	(182.8, 181.6, 185.6)	(162.4, 159.6, 152.0)	(160.0, 158.0, 172.0)	∞	(169.2, 172.6, 170.2)
5	(174.4, 170.0, 178.4)	(404.0, 428.0, 460.0)	(190.4, 172.8, 192.8)	(169.2, 172.6, 170.2)	∞
6	(176.0, 178.4, 173.6)	(293.0, 306.0, 289.0)	(46.6, 47.8, 49.0)	(164.5, 168.7, 169.6)	(53.2, 50.2, 54.2)
7	(188.8, 198.0, 187.2)	(150.8, 155.6, 144.0)	(60.6, 58.2, 59.8)	(172.0, 167.5, 175.5)	(54.8, 50.8, 44.8)
8	(176.4, 174.2, 182.8)	(172.4, 168.0, 169.2)	(65.4, 66.2, 62.8)	(165.6, 162.0, 158.6)	(64.8, 69.6, 62.4)
9	(188.6, 212.4, 220.0)	(147.4, 148.2, 144.0)	(162.8, 167.2, 168.4)	(163.2, 176.0, 164.8)	(43.6, 41.2, 40.0)
10	(220.4, 215.2, 217.2)	(157.2, 160.0, 154.2)	(216.8, 220.4, 212.0)	(217.2, 210.4, 220.4)	(54.6, 56.4, 60.2)

i/j	6	7	8	9	10
1	(176.0, 178.4, 173.6)	(188.8, 198.0, 187.2)	(176.4, 174.2, 182.8)	(188.6, 212.4, 220.0)	(220.4, 215.2, 217.2)
2	(293.0, 306.0, 289.0)	(150.8, 155.6, 144.0)	(172.4, 168.0, 169.2)	(147.4, 148.2, 144.0)	(157.2, 160.0, 154.2)
3	(46.6, 47.8, 49.0)	(60.6, 58.2, 59.8)	(65.4, 66.2, 62.8)	(162.8, 167.2, 168.4)	(216.8, 220.4, 212.0)
4	(164.5, 168.7, 169.6)	(172.0, 167.5, 175.5)	(165.6, 162.0, 158.6)	(163.2, 176.0, 164.8)	(217.2, 210.4, 220.4)
5	(53.2, 50.2, 54.2)	(54.8, 50.8, 44.8)	(64.8, 69.6, 62.4)	(43.6, 41.2, 40.0)	(54.6, 56.4, 60.2)
6	∞	(36.4, 40.8, 34.4)	(64.4, 68.8, 63.6)	(36.4, 34.0, 39.2)	(46.4, 44.8, 42.2)
7	(36.4, 40.8, 34.4)	∞	(27.2, 30.4, 32.8)	(31.6, 26.0, 23.6)	(56.8, 64.4, 60.4)
8	(64.4, 68.8, 63.6)	(27.2, 30.4, 32.8)	∞	(44.8, 38.0, 42.0)	(49.2, 55.2, 46.4)
9	(36.4, 34.0, 39.2)	(31.6, 26.0, 23.6)	(44.8, 38.0, 42.0)	∞	(67.2, 60.4, 72.8)
10	(46.4, 44.8, 42.2)	(56.8, 64.4, 60.4)	(49.2, 55.2, 46.4)	(67.2, 60.4, 72.8)	∞

Table 21
Profit vs. Risk analysis for Model- 2a.

Cases with respect to rest	Usual rest position (node)	Forced rest position (h)	Total driving duration with risk	Profit ($)	Level of risk
1	$1-\varphi 1-3$	3	0.0768	273.30	Low
2	$4-\varphi 3-2$	2	0.1357	275.20	Low
3	$5-\varphi 2-4$	4	0.4961	275.95	Low
4	$1-\varphi 1-3$				
	$4-\varphi 3-2$	3 and 2	0.2125	276.50	Low
5	$1-\varphi 1-3$				
	$5-\varphi 2-4$	3 and 4	0.5729	277.25	Medium
6	$5-\varphi 2-4$				
	$4-\varphi 3-2$	4 and 2	0.6318	279.15	Medium
7	$1-\varphi 1-3$				
	$5-\varphi 2-4$				
	$4-\varphi 3-2$	3, 4 and 2	0.7086	280.45	Medium

(0 < Low risk ≤ 0.5, 0.5 < Medium risk ≤ 1.0, 1.0 < High risk).

Table 22
Demand matrix of fruits (kg).

Retailers	1	2	3	4	5	6	7	8	9	10
Papaya	0	215	200	150	205	245	160	230	190	220
Litchi	0	150	170	250	310	250	280	285	190	275

supply (wholesaler) supplies these fruits to the retailers situated in the cities — Haldia, Burdwan, Durgapur, Asansol, Bolpur, Bankura, Purulia, Midnapore, and Kharagpur through a truck as per the retailers' demands. There are three roads connecting the cities. Total demands of the retailers are given in Table 22. As per Google's map, the distances of the roads (distance matrix) are given in Table 23 and pictorial representation is depicted in Fig. 16.

The purchasing and selling prices of Papaya and Litchi are ($ 0.54952, $ 0.68690) and ($ 0.96167, $ 1.23643), respectively. Other input parameters are the same as in Section 6.

M/s. Gazi fruit supply instructs the driver to follow a particular routing plan and appropriate routes for which profit is maximum. This problem is formulated as Model 1 and solved by the T2FLDFWA. In this case, a maximum profit of $ 440.26 is realized at 89.88 km/h. The corresponding optimal routing plan with routes is Kolkata[2]-Burdwan[2]-Bolpur[1]-Durgapur[1]-Asansol[3]-Purulia[3]-Bankura[2]-Midnapore[1]-Kharagpur[1]-Haldia[3]-Kolkata.[7] Other optimum parameters (results) are as follows: the total distance covered is 717.59 km, the total travel time is 12.968 h, the goods carrying cost is $ 411.37, the fixed carrying cost is $ 217.54, the fuel cost is $ 346.10, the fixed charge is $ 2.06, the driver salary is $ 35.63, the selling price is $ 3262.79, the total transportation cost is $ 2822.53 and no driver rest is encountered. This experiment exhibits the practical application of

[7] "Kolkata[2]-Burdwan" means the journey from Kolkata to Burdwan by route 2.

Table 23
Distance matrix for practical implementation (km).

i/j	Kolkata	Haldia	Burdwan	Durgapur	Asansol
Kolkata	∞	(119.5, 140.2, 90)	(102.9, 99.4, 120.5)	(172.3, 151.3, 148.5)	(213.2, 195.1, 236.7)
Haldia	(119.5, 140.2, 90)	∞	(197.5, 217, 180.6)	(266.4, 218.9, 297.3)	(307.3, 281.6, 327.5)
Burdwan	(102.9, 99.4, 120.5)	(197.5, 217, 180.6)	∞	(70.6, 95.4, 51.8)	(111.4, 141.8, 127.5)
Durgapur	(172.3, 151.3, 148.5)	(266.4, 218.9, 297.3)	(70.6, 95.4, 51.8)	∞	(42.7, 59.7, 61.8)
Asansol	(213.2, 195.1, 236.7)	(307.3, 281.6, 327.5)	(111.4, 141.8, 127.5)	(42.7, 59.7, 61.8)	∞
Bolpur	(165.5, 149.5, 172.7)	(259.6, 200.4, 279.1)	(59.9, 45.8, 80.6)	(56.1, 74.8, 96.8)	(96, 114.7, 81.7)
Bankura	(212.6, 185.2, 239.6)	(222.5, 195.3, 180.2)	(110.9, 94, 127.6)	(46.6, 31.2, 70.8)	(68.6, 50.7, 94.1)
Purulia	(298.7, 340.5, 254)	(301.3, 332.8, 287.1)	(197, 215.4, 187.6)	(121.6, 138.2, 105.7)	(86.9, 104.5, 70.6)
Midnapore	(131.9, 145.6, 124.5)	(117.0, 124.8, 100.7)	(207.4, 241, 192)	(153.7, 142.6, 138.2)	(175.7, 152.1, 189.4)
Kharagpur	(139, 181.6, 105.8)	(124.6, 148.1, 109.4)	(215, 231.9, 247.2)	(175.4, 155.9, 193.8)	(197.4, 217.6, 184.7)
i/j	Bolpur	Bankura	Purulia	Midnapore	Kharagpur
Kolkata	(165.5, 149.5, 172.7)	(212.6, 185.2, 239.6)	(298.7, 340.5, 254)	(131.9, 145.6, 124.5)	(139, 181.6, 105.8)
Haldia	(259.6, 200.4, 279.1)	(222.5, 195.3, 180.2)	(301.3, 332.8, 287.1)	(117.0, 124.8, 100.7)	(124.6, 148.1, 109.4)
Burdwan	(59.9, 45.8, 80.6)	(110.9, 94, 127.6)	(197, 215.4, 187.6)	(207.4, 241, 192)	(215, 231.9, 247.2)
Durgapur	(56.1, 74.8, 96.8)	(46.6, 31.2, 70.8)	(121.6, 138.2, 105.7)	(153.7, 142.6, 138.2)	(175.4, 155.9, 193.8)
Asansol	(96, 114.7, 81.7)	(68.6, 50.7, 94.1)	(86.9, 104.5, 70.6)	(175.7, 152.1, 189.4)	(197.4, 217.6, 184.7)
Bolpur	∞	(92.4, 87.4, 127.2)	(178.5, 189.4, 154.6)	(199.5, 243.8, 216.4)	(221.2, 257.4, 198.6)
Bankura	(92.4, 87.4, 127.2)	∞	(86.8, 107.4, 74.3)	(107.8, 90.1, 129.2)	(129.4, 151.7, 109.5)
Purulia	(178.5, 189.4, 154.6)	(86.8, 107.4, 74.3)	∞	(186.6, 162.6, 150.8)	(203.3, 234.1, 185.6)
Midnapore	(199.5, 243.8, 216.4)	(107.8, 90.1, 129.2)	(186.6, 162.6, 150.8)	∞	(24, 39.4, 45.9)
Kharagpur	(221.2, 257.4, 198.6)	(129.4, 151.7, 109.5)	(203.3, 234.1, 185.6)	(24, 39.4, 45.9)	∞

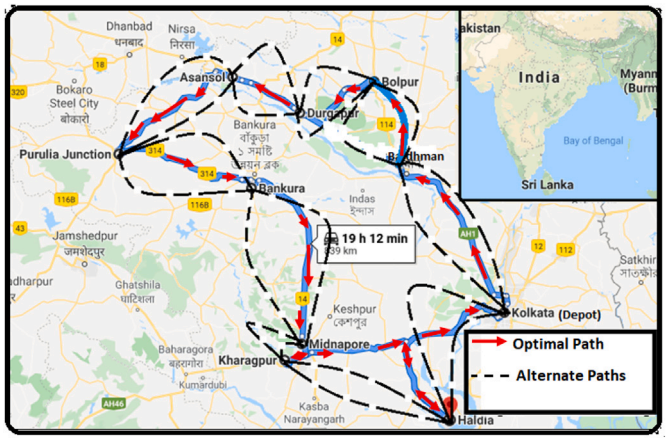

Fig. 16. Route map of fruits distribution by M/s. Gazi fruit supply.

the proposed model and the efficiency of the proposed metaheuristic algorithm (T2FLDFWA).

This investigation presents how management should make optimal decisions to maximize overall profit in a fresh fruit delivery system while keeping total costs and emissions as low as possible. It is seen that the selection of the routing plan and the corresponding routes are crucial (Section 7.5). Moreover, management can decide depending on how much importance is given to profit and CSR wrt. environment. If profit is the only goal, then Model 1 can be adopted. If environmental awareness is given maximum priority, Model-5 can be used, and for a compromised solution, Model-6 can be adopted, showing the different weights of importance to the profit and environmental pollution. Again, for minimum environmental pollution and minimum total cost, Section 7.3 can be referenced. If the management desires to have more profit with some continuous driving risk, Section 7.7 can be followed, and Table 19 can be referred to. All these results are wrt. freshness function $H_1^k(T_i)$ and average travel velocity for the entire tour. Management can easily evaluate the other models with the different freshness functions following the steps of Model 1.

9. Conclusion and future scope

A twofold investigation is conducted in this study, i.e., (i) formulation of a realistic multiroute (3D) green fresh fruit distribution model for maximum profit, minimum fuel cost, and a compromise between these two, and (ii) development of fast and efficient heuristic solution methodologies for TSP-type NP-hard problems are presented. From this analysis, a wholesaler can estimate the total time and expenditure requirement to maximize the overall profit (which is the main goal of a company/organization) or to fulfill social commitment (CSR) wrt. environment or a compromise. Two algorithms, T1FLDFWA and T2FLDFWA, have been developed and tested against some standard problems, and T2FLDFWA is used to solve the proposed model. For comparison, ANOVA is used, and the results show the supremacy of the T2FLDFWA.

The main objective of the proposed model is to suggest an optimum distribution plan for a fresh produce selling company to have maximum possible profit and to perform the CSR wrt. environment.

A trade-off between profit and fuel cost is illustrated. For the first time, 3D routing, i.e., routing with the availability of different routes between nodes, routing with a time-dependent freshness function for fresh products and green consideration, the introduction of a realistic new freshness function, the inclusion of driver fatigue, routing with driver rest, and profit against some risks are illustrated. These innovations and concepts can be applied to other routing problems, such as TPP and medicine distribution to health centers. Here, new DFWAs, i.e., T1FLDFWA and T2FLDFWA, have been developed in general form to solve TSP-type NP-hard problems. Therefore, these can be used to solve covering salesman problems, VRPs, facility location problems, etc.

The limitations of the present investigation are as follows:

Roads with different lengths between the nodes are considered, but road specifications, roughness and congestion, etc., on which travel velocity depends, are not taken into account. The scaling of risks for continuous driving can be more data-specific and expressed in a fuzzy sense. Recently, refrigerated vehicles/containers have been used for the long-distance transportation/distribution of perishable items. The effects of the refrigeration on the item's freshness should be defined and considered.

For future extensions, the above limitations can be removed to make the model more realistic. Moreover, weather conditions, visibility, etc., can be considered to calculate travel velocity and continuous driving risk. For this purpose, Internet of Things devices can be used to obtain information from the cloud. However, due to the imprecise information, fuzzy/rough sets can be used to address uncertainties. In some cases, during unloading, the driver is supposed to be on the wheel. Retailers may ask for delivery within a specific time period (Time window); otherwise, the wholesaler will have to pay some penalties.

Currently, customer satisfaction is prioritized in many distribution systems. Therefore, in the present investigation, customers' satisfaction wrt. time windows for delivery, specified/preferred freshness of the items, etc., can be introduced as constraints or an objective. As mentioned, for perishable items transported through refrigerated vehicles, rot is delayed. Again, this process invites more CE in addition to the usual CE from the vehicle. The minimization/control of CE may also be considered for future work. To validate the T2FLDFWA, a more detailed analysis, including some other established tests, can be performed.

CRediT authorship contribution statement

Kishore Thakur: Conceptualization, Methodology, Software, Data curation, Writing – original draft. **Somnath Maji:** Data curation, Writing – Original draft, Writing – review & editing. **Samir Maity:** Software, Validation, Data curation, Visualization, Investigation. **Tandra Pal:** Supervision, Editing. **Manoranjan Maiti:** Conceptualization, Writing – review & editing.

Declaration of competing interest

The authors declare that they have no known competing financial interests or personal relationships that could have appeared to influence the work reported in this paper.

Data availability

Data will be made available on request.

Appendix A. Supplementary data

Supplementary material related to this article can be found online at https://doi.org/10.1016/j.eswa.2023.120300.

References

Abdulmajeed, N. H., & Ayob, M. (2014). A firework algorithm for solving capacitated vehicle routing problem. *International Journal of Advancements in Computing Technology*, *6*(1), 79.

Altinoz, O. T., & Yilmaz, A. E. (2019). Multiobjective Hooke–Jeeves algorithm with a stochastic Newton–Raphson-like step-size method. *Expert Systems with Applications*, *117*, 166–175.

Babagolzadeh, M., Shrestha, A., Abbasi, B., Zhang, Y., Woodhead, A., & Zhang, A. (2020). Sustainable cold supply chain management under demand uncertainty and carbon tax regulation. *Transportation Research Part D: Transport and Environment*, *80*, Article 102245.

Barraza, J., Melin, P., Valdez, F., & Gonzalez, C. I. (2016). Fuzzy FWA with dynamic adaptation of parameters. In *2016 IEEE congress on evolutionary computation* CEC, (pp. 4053–4060). IEEE.

Barraza, J., Melin, P., Valdez, F., & Gonzalez, C. (2017). Fuzzy fireworks algorithm based on a sparks dispersion measure. *Algorithms*, *10*(3), 83.

Barth, M., & Boriboonsomsin, K. (2009). Energy and emissions impacts of a freeway-based dynamic eco-driving system. *Transportation Research Part D: Transport and Environment*, *14*(6), 400–410.

Bektaş, T., & Laporte, G. (2011). The pollution-routing problem. *Transportation Research, Part B (Methodological)*, *45*(8), 1232–1250.

Blackburn, J., & Scudder, G. (2009). Supply chain strategies for perishable products: the case of fresh produce. *Production and Operations Management*, *18*(2), 129–137.

Bozanic, D., Tešić, D., Marinković, D., & Milić, A. (2021). Modeling of neuro-fuzzy system as a support in decision-making processes. *Reports in Mechanical Engineering*, *2*(1), 222–234.

Branke, J., Branke, J., Deb, K., Miettinen, K., & Slowiński, R. (2008). *Multiobjective optimization: Interactive and evolutionary approaches, Vol. 5252*. Springer Science & Business Media.

Çam, Ö. N., & Sezen, H. K. (2020). The formulation of a linear programming model for the vehicle routing problem in order to minimize idle time. *Decision Making: Applications in Management and Engineering*, *3*(1), 22–29.

Castillo, O., Amador-Angulo, L., Castro, J. R., & Garcia-Valdez, M. (2016). A comparative study of type-1 fuzzy logic systems, interval type-2 fuzzy logic systems and generalized type-2 fuzzy logic systems in control problems. *Information Sciences*, *354*, 257–274.

Chen, J., Dong, M., & Xu, L. (2018). A perishable product shipment consolidation model considering freshness-keeping effort. *Transportation Research Part E: Logistics and Transportation Review*, *115*, 56–86.

Dai, Z., Gao, K., & Giri, B. (2020). A hybrid heuristic algorithm for cyclic inventory-routing problem with perishable products in VMI supply chain. *Expert Systems with Applications*, *153*, Article 113322.

Das, S. K., & Roy, S. K. (2019). Effect of variable carbon emission in a multi-objective transportation-p-facility location problem under neutrosophic environment. *Computers & Industrial Engineering*, *132*, 311–324.

Das, M., Roy, A., Maity, S., Kar, S., & Sengupta, S. (2021). Solving fuzzy dynamic ship routing and scheduling problem through new genetic algorithm. *Decision Making: Applications in Management and Engineering*.

De, M., & Giri, B. (2020). Modelling a closed-loop supply chain with a heterogeneous fleet under carbon emission reduction policy. *Transportation Research Part E: Logistics and Transportation Review*, *133*, Article 101813.

Demir, E., Bektaş, T., & Laporte, G. (2014). A review of recent research on green road freight transportation. *European Journal of Operational Research*, *237*(3), 775–793.

Dorigo, M., Colorni, A., & Maniezzo, V. (1991). Distributed optimization by ant colonies.

Gao, X., Hu, X., Han, J., Huo, X., Zhu, Y., Liu, T., & Ruan, J. (2020). A network flow model of regional transportation of E-commerce and analysis on maturity change of fresh fruit. *International Journal of Innovative Computing, Information and Control*, *16*, 955–972.

Garnier, S., Gautrais, J., & Theraulaz, G. (2007). The biological principles of swarm intelligence. *Swarm Intelligence*, *1*(1), 3–31.

Ghosh, S., Roy, S. K., & Fügenschuh, A. (2022). The multi-objective solid transportation problem with preservation technology using pythagorean fuzzy sets. *International Journal of Fuzzy Systems*, *24*(6), 2687–2704.

Giri, B. K., & Roy, S. K. (2022). Neutrosophic multi-objective green four-dimensional fixed-charge transportation problem. *International Journal of Machine Learning and Cybernetics*, *13*(10), 3089–3112.

Gokarn, S., & Kuthambalayan, T. S. (2019). Creating sustainable fresh produce supply chains by managing uncertainties. *Journal of Cleaner Production*, *207*, 908–919.

Guendouz, M., Amine, A., & Hamou, R. M. (2017). A discrete modified fireworks algorithm for community detection in complex networks. *Applied Intelligence*, *46*(2), 373–385.

Gustavsson, J., Cederberg, C., Sonesson, U., Otterdijk, R., & Meybeck, A. (2011). *Interpack 2011*. Food and Agriculture Organization of the United Nations.

Janecek, A., & Tan, Y. (2011). Using population based algorithms for initializing nonnegative matrix factorization. In *International conference in swarm intelligence* (pp. 307–316). Springer.

Jedermann, R., Nicometo, M., Uysal, I., & Lang, W. (2014). Reducing food losses by intelligent food logistics.

Jouzdani, J., & Govindan, K. (2021). On the sustainable perishable food supply chain network design: A dairy products case to achieve sustainable development goals. *Journal of Cleaner Production*, *278*, Article 123060.

Jovanović, A., & Teodorović, D. (2022). Type-2 fuzzy logic based transit priority strategy. *Expert Systems with Applications*, *187*, Article 115875.

Kennedy, J., & Eberhart, R. (1995). Particle swarm optimization. In *Proceedings of ICNN'95-International conference on neural networks, Vol. 4* (pp. 1942–1948). IEEE.

Khalilpourazari, S., & Khalilpourazary, S. (2019). An efficient hybrid algorithm based on Water Cycle and Moth-Flame Optimization algorithms for solving numerical and constrained engineering optimization problems. *Soft Computing*, *23*(5), 1699–1722.

Kıran, M. S., Özceylan, E., Gündüz, M., & Paksoy, T. (2012). A novel hybrid approach based on particle swarm optimization and ant colony algorithm to forecast energy demand of Turkey. *Energy Conversion and Management*, *53*(1), 75–83.

Krishna, M. M., Panda, N., & Majhi, S. K. (2021). Solving traveling salesman problem using hybridization of rider optimization and spotted hyena optimization algorithm. *Expert Systems with Applications*, Article 115353.

Kuzmanović, M., & Vukić, M. (2021). Incorporating heterogeneity of travelers' preferences into the overall hostel performance rating. *Decision Making: Applications in Management and Engineering*, *4*(2), 200–224.

Lawler, E. L. (1985). *Wiley-interscience series in discrete mathematics*, *The traveling salesman problem: a guided tour of combinatorial optimization*.

Liao, W., Zhang, L., & Wei, Z. (2020). Multi-objective green meal delivery routing problem based on a two-stage solution strategy. *Journal of Cleaner Production*, *258*, Article 120627.

Liu, X., & Qin, X. (2021). A neighborhood information utilization fireworks algorithm and its application to traffic flow prediction. *Expert Systems with Applications*, *183*, Article 115189.

Maity, S., Roy, A., & Maiti, M. (2016). An imprecise multi-objective genetic algorithm for uncertain constrained multi-objective solid travelling salesman problem. *Expert Systems with Applications*, *46*, 196–223.

Mardani, A., Kannan, D., Hooker, R. E., Ozkul, S., Alrasheedi, M., & Tirkolaee, E. B. (2020). Evaluation of green and sustainable supply chain management using structural equation modelling: A systematic review of the state of the art literature and recommendations for future research. *Journal of Cleaner Production*, *249*, Article 119383.

Micheli, G. J., & Mantella, F. (2018). Modelling an environmentally-extended inventory routing problem with demand uncertainty and a heterogeneous fleet under carbon control policies. *International Journal of Production Economics*, *204*, 316–327.

Mitra, S., & Pathak, P. (2008). Litchi production in the Asia-Pacific region. In *III international symposium on longan, lychee, and other fruit trees in sapindaceae family 863* (pp. 29–36).

Ontiveros-Robles, E., Castillo, O., & Melin, P. (2021). Towards asymmetric uncertainty modeling in designing General Type-2 Fuzzy classifiers for medical diagnosis. *Expert Systems with Applications*, *183*, Article 115370.

Özmen, A., Kropat, E., & Weber, G.-W. (2017). Robust optimization in spline regression models for multi-model regulatory networks under polyhedral uncertainty. *Optimization*, *66*(12), 2135–2155.

Paul, A., Pervin, M., Roy, S. K., Maculan, N., & Weber, G.-W. (2022). A green inventory model with the effect of carbon taxation. *Annals of Operations Research*, *309*(1), 233–248.

Poonthalir, G., & Nadarajan, R. (2018). A fuel efficient green vehicle routing problem with varying speed constraint (F-GVRP). *Expert Systems with Applications*, *100*, 131–144.

Raghuram, G. (2012). Evolution of model concession agreement for national highways in India. *National*.

Rohmer, S., Claassen, G., & Laporte, G. (2019). A two-echelon inventory routing problem for perishable products. *Computers & Operations Research*, *107*, 156–172.

Sanchez, M. A., Castillo, O., & Castro, J. R. (2015). Generalized type-2 fuzzy systems for controlling a mobile robot and a performance comparison with interval type-2 and type-1 fuzzy systems. *Expert Systems with Applications*, *42*(14), 5904–5914.

Scora, G., & Barth, M. (2006). *Comprehensive modal emissions model (cmem), version 3.01, Vol. 1070*. Riverside: User Guide. Centre for Environmental Research and Technology. University of California.

Soon, K. L., Lim, J. M.-Y., Parthiban, R., & Ho, M. C. (2019). Proactive eco-friendly pheromone-based green vehicle routing for multi-agent systems. *Expert Systems with Applications*, *121*, 324–337.

Sun, Z., Wang, N., & Bi, Y. (2015). Type-1/type-2 fuzzy logic systems optimization with RNA genetic algorithm for double inverted pendulum. *Applied Mathematical Modelling*, *39*(1), 70–85.

Tan, Y. (2015). Discrete firework algorithm for combinatorial optimization problem. In *Fireworks algorithm* (pp. 209–226). Springer.

Tan, Y., & Zhu, Y. (2010). Fireworks algorithm for optimization. In *International conference in swarm intelligence* (pp. 355–364). Springer.

Tucker, P., Folkard, S., & Macdonald, I. (2003). Rest breaks and accident risk. *The Lancet*, *361*(9358), 680.

Wang, S., Liu, M., & Chu, F. (2020). Approximate and exact algorithms for an energy minimization traveling salesman problem. *Journal of Cleaner Production*, *249*, Article 119433.

Wang, L., & Pei, Y. (2014). The impact of continuous driving time and rest time on commercial drivers' driving performance and recovery. *Journal of Safety Research*, *50*, 11–15.

Wang, X., Sun, X., Dong, J., Wang, M., & Ruan, J. (2017). Optimizing terminal delivery of perishable products considering customer satisfaction. *Mathematical Problems in Engineering*, *2017*.

Wang, Y., Zhang, J., Guan, X., Xu, M., Wang, Z., & Wang, H. (2021). Collaborative multiple centers fresh logistics distribution network optimization with resource sharing and temperature control constraints. *Expert Systems with Applications*, *165*, Article 113838.

Xie, S., Xie, Y., Li, F., Jiang, Z., & Gui, W. (2019). Hybrid fuzzy control for the goethite process in zinc production plant combining type-1 and type-2 fuzzy logics. *Neurocomputing*, *366*, 170–177.

Zheng, Y.-J., Xu, X.-L., Ling, H.-F., & Chen, S.-Y. (2015). A hybrid fireworks optimization method with differential evolution operators. *Neurocomputing*, *148*, 75–82.

Zhuang, Y., Sun, Y., Yu, M., & Hu, X. (2019). A path selection model for multimodal transportation problem of fresh fruits in online supermarket. *ICIC Express Letters*, *13*(3), 201–208.